Multimedia Tools and Applications (2021) 80:12435–12468
https://doi.org/10.1007/s11042-020-10313-w

Multilevel thresholding image segmentation based on improved volleyball premier league algorithm using whale optimization algorithm

Mohamed Abd Elaziz[1] · Neggaz Nabil[2] · Reza Moghdani[3] · Ahmed A. Ewees[4] · Erik Cuevas[5] · Songfeng Lu[6]

Received: 15 October 2019 / Revised: 26 August 2020 / Accepted: 22 December 2020 /
Published online: 11 January 2021

Abstract
Multilevel thresholding image segmentation has received considerable attention in several image processing applications. However, the process of determining the optimal threshold values (as the preprocessing step) is time-consuming when traditional methods are used. Although these limitations can be addressed by applying metaheuristic methods, such approaches may be idle with a local solution. This study proposed an alternative multilevel thresholding image segmentation method called VPLWOA, which is an improved version of the volleyball premier league (VPL) algorithm using the whale optimization algorithm (WOA). In VPLWOA, the WOA is used as a local search system to improve the learning phase of the VPL algorithm. A set of experimental series is performed using two different image datasets to assess the performance of the VPLWOA in determining the values that may be optimal threshold, and the performance of this algorithm is compared with other approaches. Experimental results show that the proposed VPLWOA outperforms the other approaches in terms of several performance measures, such as signal-to-noise ratio and structural similarity index.

Keywords Image segmentation · Multilevel thresholding · Swarm algorithm · Volleyball premier league algorithm · Whale optimization algorithm

1 Introduction

The segmentation is a fundamental and crucial step in image processing and artificial vision. A significant number of applications explored the process of segmentation, such as medical imaging [29], video semantic [38], script identification [26], historical documents [51], and

✉ Mohamed Abd Elaziz
abd_el_aziz_m@yahoo.com

✉ Songfeng Lu
lusongfeng@hust.edu.cn

Extended author information available on the last page of the article

remote sensing [47]. Segmentation is defined as an operation that partitions the image into several homogeneous objects. Mainly, the segmentation image includes several techniques such as thresholding, edge detection, split and merge method, and region growing [47].

Among the methods mentioned above, thresholding is the most used and exploited due to its efficiency and more straightforward implementation. Typically, two variants of thresholding are widely used in the literature known as binary thresholding (bi-level) and multilevel thresholding (ML-TH). The main idea of binary thresholding is to find the optimal value of threshold (T), which aims to create two classes by comparing the pixel intensity to T. The lower values are affected to the first class while the higher values are assigned to the second class.

Generally, ML-TH is the most exploited in image processing because the number of classes is more significant than the two classes. Besides, this type requires several values of thresholds. The main problem of thresholding is how to find automatically the optimal value of threshold(s), which leads to determining the number of clusters (classes) correctly.

For binary thresholding, we distinguish two strategies. The first one is introduced by Otsu in [36] that aimed to maximize the variance between classes. The second strategy is provided by Kapur [24] that used the entropy criteria as a measure to maximize the homogeneity between classes.

For ML-TH, a new class of metaheuristic algorithms based on genetic evolution, swarm theory, and physical laws have been applied. Several methods, such as genetic algorithm (GA) [45], differential evolution (DE) [41], particle swarm optimization (PSO) [2], multi-verse optimizer (MVO) [11], artificial bee colony (ABC) [14], artificial bee colony (ABC) [18], chicken swarm optimization [28], electromagnetism optimization [34], and gravitational search algorithm (GSA) [31], are available in the literature. They are applied to obtain the optimal set of thresholding by maximizing the interclass variance defined by Otsu's function.

Recently, the intention of scientific is attracted by the simulation of the natural behavior of insects and animals, which increase the development of several algorithms. We find the work of Farshi in [16] that introduced a novel technique named animal migration optimize for finding the optimal set of multiple thresholds. The author used two criteria most exploited in the field of image thresholding known as Kapur entropy and Otsu method. The experimental study showed better results in comparison with other optimization algorithms such as GA, PSO, and BFO. In [7], the authors proposed three heuristics based ML- thresholding, namely OA-TH, PSO-TH, and GWO-TH, for selecting the optimal thresholds. The authors used the Otsu method to maximize the between-class variance. The experimental results demonstrated the high performance of WOA-TH compared to GWO-TH and PSO-TH.

In the same context, in Ref [22], the authors proposed a novel enhanced version of bee algorithms (BAs) to multilevel image thresholding, called PLBA. This algorithm aimed to determine the optimal values of the threshold by maximizing between class-variance and Kapur's entropy. Besides, this algorithm included two searches (i.e., local and global). The first one applied the greedy Levy local algorithm [39], which is based on the levy flight operator. Also, the global search incorporated the path levy in the initialization phase that is used in PLBA. The PLBA outperformed other metaheuristic algorithms.

A new approach to multilevel thresholding based on GWO is developed by [25]. The researchers imitated the social life of wolves, which usually depended on their leadership hierarchy and hunting activities. The proposed method selected the optimal threshold values using the criteria of Kapur's entropy or Otsu's between-class variance. The experimental results showed that the GWO provided an excellent performance over BFO and PSO.

Moreover, the computational complexity of GWO is greatly diminished because it was faster than the BFO.

Mohamed et al. [9] proposed two algorithms based on swarm intelligence, called whale optimization algorithm (WOA) and moth-flame optimization (MFO), for multilevel threshold segmentation. The WOA emulated the natural cooperative behavior of whales, whereas the MFO mimicked the behavior of moths, which have a unique navigation style at night based on the moonlight. Otsu's between-class variance evaluates the fitness function, and the experimental result showed that MFO provided a better result than WOA.

The authors of [4] developed a novel multilevel thresholding algorithm based on swarm intelligence theory, called krill herd optimization (KHO), which simulates the herding behavior of krill agents. This study introduced the KHO to find the optimal threshold values of image segmentation by maximizing the Kapur and Otsu measures. A comparative study showed that the proposed method outperformed other existing bio-inspired approaches, such as GA, MFO, and PSO.

The segmentation of color images has recently grown remarkably in image processing. A new method has been proposed [20], which presented an improved version of the FA, called MFA, by minimizing cross-entropy, intra-class variance, and Kapur's method. The main difference between MFA and FA resided in the initialization and movement phase. The initialization phase is conducted by a chaotic map, which improved the diversification and convergence, whereas the phase of the movement is based on PSO.

Physical and mathematical theories attracted the attention of researchers, which allows to develop several algorithms for MLT. This category included sine cosine algorithm (SCA) [19], Multiverse optimizer (MVO) [23], Electro-magnetism (EM) [6], Equilibrium Optimizer (EO) [48] and Gravitational Search Algorithm [44].

Physical rules are considered as a new source for studying the ML-TH, for example Xing and Jia [49] proposed a multi-threshold image segmentation based on grey level co-occurrence matrix (GLCM) and improved Thermal exchange optimize (TEO) using two operators: levy flight and oppsition-based-learning (OBL). To validate the efficiency of the proposed method, natural-color image, satellite image, and Berkeley images are taken as an experiment. GLCM-ITEO has shown a high quality of segmentation with less CPU time.

An improved thermal exchange optimization using a levy flight function is proposed [50]. For validating the efficiency of LTEO, six swarms are used for comparison tested on color nature image and satellite image. The experimental study has shown high accuracy of segmentation and speed convergence.

Recently, the use of the volleyball premier league (VPL) algorithm proposed by Moghdani et al. [32] is a known great success for solving global optimization problems. In general, the VPL consists of applying several strategies inspired by a volleyball game, which are used to improve the population during the seasons. The VPL showed some difficulties in terms of convergence and local optima. So, the learning phase has the most substantial effect on the performance of the VPL algorithm. To avoid the problem of convergence and to enhance the learning phase, we integrate the whale optimization algorithm (WOA), which is used as a local search.

In general, the WOA emulated the behavior of whales during the searching for prey [30]. The WOA has been applied to different applications based on these characteristics (e.g., economic dispatch problem [46], bioinformatics [3], feature selection [42], and content-based image retrieval [10]).

The main contributions of this paper are:

- For the first time, the sports inspiration based on basic VPL is applied for multilevel thresholding
- A new hybrid algorithm called VPLWOA is developed for selecting the optimal threshold values on various images by maximizing the between class-variance defined by Otsu's function.
- Assess the quality of the proposed VPLWOA using eleven natural images that have different properties.
- A new real application of blood cell segmentation based on VPLWOA is realized to find the optimal thresholds.
- Experimental results show that VPLWOA outperforms other different metaheuristic algorithms in terms of performance criteria.

The general structure of the paper takes the form of five chapters. Image segmentation using Otsu's function, the VPL algorithm, and the WOA are described in Section 2. The proposed method (i.e., VPLWOA) is explained in Section 3. A comprehensive evaluation of our method with a statistical study of various images is presented in Section 4. Finally, our conclusion and future work are discoursed in Section 5.

2 Related work

Recently, many studies are explored by the researcher for understanding the behavior of the life cycle of insects, animals, and nature or physical theory. These inspirations lead deeply to appear several thresholding algorithms inspired from genetic as evolutionary algorithms. More recently, the swarm intelligence family still more attractive with the simulation of insects and animal's life including harris hawks, ant lion, whales grey wolves, salps, ant's colonies, bees. In this side, several algorithms are introduced for multilevel thresholding images including Harris hawk's optimizer, grey wolf optimizer, ant colony optimization, artificial bee colony ant lion optimizer, whale optimization algorithm, salp swarm algorithm.

Recently, Eric et al. [40] introduced an efficient swarm optimizer called harris hawks optimizer (HHO) for solving multilevel thresholding based on minimum cross-entropy. The authors treat the standard benchmark of images and medical mammograms. The proposed method is shown their efficiency compared to basic machine learning and metaheuristics approaches, including PSO, FFA, DE, HS, SCA, and ABC in terms of PSNR, FSIM, SSIM, PRI, and VOL. In addition, HHO consumed less time compared to PSO, FFA, and DE.

In this literature review, we give more importance to segmentation images based on hybrid metaheuristics. For example, Abdelaziz et al. [12] developed a new hybrid algorithm based on the HHO and salp swarm algorithm (SSA) for finding the optimal values of the multilevel threshold. The general idea consists of dividing the population into two parts, where the process of exploration and exploitation of HHO is applied to the first part, and the searching process of SSA is used for updating the solutions of the second part. The proposed method HHOSSA achieved high performance compared to original versions of HHO and SSA in terms of PSNR and SSIM, tested on natural gray-level images.

Ahmadi et al. [1] proposed a hybrid algorithm for seeking the optimal values of the level threshold using differential evolution (DE) and bird mating optimization (BMA). The numerical results have shown the high performance of the proposed method assessed on standard test images and compared to other optimizers like PSO, PSO-DE, GA, Bacterial foraging (BF), and enhanced BF in terms of fitness and standard deviation.

In the same context of MLT segmentation image based on hybrid metaheuristics, a new combination between Spherical search optimizer (SSO) and sine cosine algorithm (SCA) is developed by Husein et al. [33]. The fuzzy entropy is considered as the main fitness function for testing the quality of the segmented image. The experimental study is assessed on several images taken from Berkeley datasets and the obtained results of SSOSCA outperformed other optimizer that included Cuckoo search (CS), Grey wolf optimizer (GWO), WOA, SCA, SSA, SSO, GOA over different performance metrics as PSNR, FSIM, and SSIM. The proposed method took a lower time for achieving the segmentation task compared to other optimizers.

In [5], The authors introduced a new hybrid algorithm called HHO-DE for MLT color segmentation image. Their idea consists of dividing [5] firstly the main population into two equal subpopulations. Secondly, HHO and DE update the position of each subpopulation in a parallel way. Two fitness functions are used based on Otsu and Kapur entropy to determine the optimal set of threshold levels. The experimental results indicated that HHO-DE could be considered as an efficient tool for MLT color image segmentation compared to other optimizers as DE HHO SCA BA HSO PSO DA according to PSNR SSIM and FSIM measures.

With the fast propagation of COVID-19, several researchers presented many solutions for the detection and segmentation of chest CT gray-level images. In [13], the authors proposed a new version of the marine predator's algorithm (MPA) improved by MFO based on fuzzy entropy. The proposed method MPAMFO presented their efficiency compared to the existing swarm intelligence works in terms of PSNR and SSIM.

Sun et al. [43] introduced an algorithm called GSA-GA, which combined GSA with a genetic technique for multilevel thresholding. This algorithm used the roulette selection and mutation operator inspired by genetic technique, which is integrated into GSA. Two standard criteria (i.e., entropy and between-class variance) are used as fitness functions. The statistical significance test demonstrated that GSA-GA considerably diminished the computational complexity of all images tested.

Furthermore, Oliva et al. [35] proposed a new evolutionary algorithm that combines Antlion optimization and a sine-cosine algorithm to determine the optimal set of thresholding segmentation using Otsu's between-class variance and Kapur's entropy. According to the experimental study, the SCA does not outperform other evolutionary computation from state of the art.

Ouadfel and Taleb-Ahmed [37] investigated the ability of two nature-inspired metaheuristics, called social spiders optimization (SSO) and flower pollination (FP) to solve the image segmentation via multilevel thresholding. During the optimization process, each solution is evaluated using the between-class variance or Kapur's entropy. The experimental results illustrated that the SSO and FP better than PSO and bat algorithms. Furthermore, the SSO guaranteed a balance between exploration and exploitation and showed the stability of results for all images.

3 Background

In this section, the necessary information of the multilevel thresholding image segmentation using Otsu's function, VPL, and WOA are discussed.

3.1 Problem formulation

In this section, the definition of the multilevel thresholding problem is explained. Assumed that the tested image I contains a set of $K+1$ classes, and a set of K threshold values (t_k, $k=1, 2\ldots, K$) are required to divide I into these classes (C_k, $k=1, 2\ldots, K$). This condition can be represented by the following equation [37]:

$$\begin{aligned} C_0 &= \left\{ I_{ij} \in I \middle| 0 \le I_{ij} \le t_1 - 1 \right\}, \\ C_1 &= \left\{ I_{ij} \in I \middle| t_1 \le I_{ij} \le t_2 - 1 \right\}, \\ &\cdots \\ C_K &= \left\{ I_{ij} \in I \middle| t_K \le I_{ij} \le L - 1 \right\} \end{aligned} \tag{1}$$

where L is the gray level of I.

In general, the task of determining the optimal threshold values to segment the image is by conversion to an optimization problem through maximizing or minimizing a specific objective function. We suppose the maximization in this paper, which is defined as follows:

$$t_1^*, t_2^*, \ldots, t_K^* = \max_{t_1, t_2, \ldots, t_K} F(t_1, t_2, \ldots, t_K), \tag{2}$$

Where F is the objective function used to evaluate each solution. In the following sections, the most popular two functions used in the multilevel threshold image segmentation are defined.

3.2 Otsu's method

In [36], the description of the Otsu's method was given. This method aims to maximize the variance between the classes of the given image I using the following equation:

$$F_{Otsu} = \sum_{i=0}^{K} \theta_i \times (\mu_i - \mu_1)^2, \quad \theta_i = \sum_{j=t_i}^{t_{i+1}-1} P_j, \tag{3}$$

$$\mu_i = \sum_{j=t_i}^{t_{i+1}-1} \frac{iP_j}{\theta_j}, \quad P_i = \frac{Fr_i}{N_p}, \quad t_0 = 0, t_{K+1} = L, \tag{4}$$

where μ_1 is the mean intensity of the image I; and P_i and Fr_i are the probability and frequency of the ith gray level of the image, respectively. The total number of pixels in the image is given by N_p.

3.3 Volleyball premier league algorithm

This subsection is demonstrated the mathematical modeling of the proposed algorithm, Volleyball Premier League algorithm (VPL) [32], which is explained comprehensively.

The general flow of VPL is presented in Fig. 1, including all steps of the proposed algorithm.

In this algorithm, we use two parts that contain formation and substitutes for each solution, wherein random numbers are used in the identified interval values, as shown in Eqs. (5) moreover, (6) [32]:

$$X_j^f = lb_j + Rand() \times \left(ub_j - lb_j\right) \tag{5}$$

$$X_j^s = lb_j + Rand() \times \left(ub_j - lb_j\right) \tag{6}$$

where lb_j and ub_j denote the range of variable j, respectively; and $Rand()$ is a random number generated between zero and one. In the VPL algorithm, we perform a well-known procedure, which is named single round robin (SRR), to provide the league's schedule.

In the typical volleyball game, the better team can beat its rival in the match. Each team has a chance of running up against its competitors according to the probability rules in the match. The power index $\pi(i)$ is defined on the basis of the following formulas:

$$\pi(i) = \frac{f\left(X_i^f\right)}{Z}, \tag{7}$$

$$Z = \sum_{i=1}^{n} f\left(X_i^f\right), \tag{8}$$

In the above formulas, $f\left(X_i^f\right)$ denotes the objective function of the ith team, which is calculated based on its formation property; Z denotes the summation of the objective function

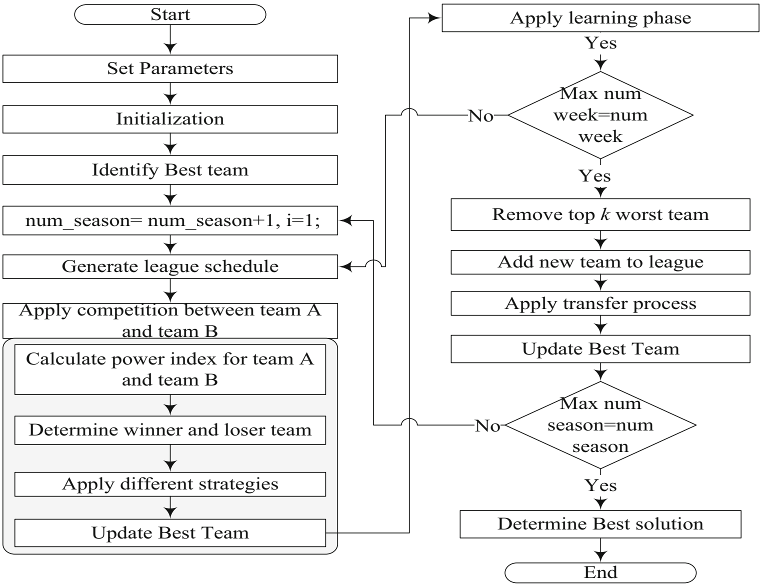

Fig. 1 The framework of the VPL algorithm

in the current iteration. Moreover, the following formulations are given to compute the π value for both teams, which are going to play each other in this match.

$$\pi(j) = \frac{f\left(X_j^f\right)}{Z} \tag{9}$$

$$\pi(k) = \frac{f\left(X_k^f\right)}{Z} \tag{10}$$

where X_j^f and X_k^f denote the position of formation property of teams j and k, respectively. Therefore, we can compute the probability of winning team j against k with the following formula:

$$\rho(j,k) = \frac{\pi(j)}{\pi(j) + \pi(k)} \tag{11}$$

According to the laws of probability, the following formula is given as:

$$\rho(j,k) + \rho(k,j) = 1 \tag{12}$$

A new formation and corresponding strategies are used for the winner and loser teams, considering that the winning team is determined. In this regard, different operators, including knowledge sharing, repositioning, and substitution, are used for the loser team, and the winning team operates the leading role strategy. Generally, the coach shares his knowledge about the condition of the game with players to obtain improved performance. Thus, knowledge sharing strategy can be specified by:

$$X_j^f(t+1) = X_j^f(t) + r_1 \lambda^f \left(ub_j - lb_j\right), \tag{13}$$

$$X_j^s(t+1) = X_j^s(t) + r_2 \lambda^s \left(ub_j - lb_j\right), \tag{14}$$

In the above formulas, we have defined coefficients values (λ^f andλ^s) for formation and substitutes properties; and also, two new random numbers, which are indicated r_1 and r_2, are uniformly engendered in range zero to one. Furthermore, the rate of sharing knowledge is indicated by δ_{ks} which is computed as follows:

$$N_{ks} = [J\delta_{ks}], \tag{15}$$

where N_{ks} denotes the amount of knowledge sharing for any solution, and J is considered as the amount of positions in solutions. Repositioning is a common strategy, which has considerable effects on a volleyball game during a match. This operator positions the best players in the ideal to attain excellent performance. On this basis, we mention δ_{rs} as the rate of repositioning procedure, and the number of this operator in the current iteration is given as:

$$N_{rs} = [J\delta_{rs}], \tag{16}$$

where N_{ks} states the number of this operator in each iteration. At this point, we randomly select two positions (i.e., i and j), and α and β (two virtual objects) are used for storing the value of active and passive players, respectively. Then, the properties of solutions i and j to are assigned to α and β. Therefore, the following formulas are given:

$$\alpha^f = X_i^f, \tag{17}$$

$$\alpha^s = X_i^s, \tag{18}$$

$$\beta^f = X_j^f, \tag{19}$$

$$\beta^s = X_j^s. \tag{20}$$

At the end of this process, the following formulas are given, which are indicated that properties of selected positions (*A* and *B*) are assigned to each other reversely.

$$X_i^f = \beta^f, \tag{21}$$

$$X_i^s = \beta^s, \tag{22}$$

$$X_j^f = \alpha^f, \tag{23}$$

$$X_j^s = \alpha^s. \tag{24}$$

We can increase our knowledge in performing the corresponding operators in this algorithm by understanding the similarities and differences among sports. Therefore, the coaches use substitution for the intervention to find the best formation for their teams. The number of substitution (N_s) in each iteration is calculated by the following formula::

$$N_s = [rJ], \tag{25}$$

Where r represents a random number that is distributed uniformly between zero and one, and J specifies the dimension of each solution, which is identified as the number of players in this algorithm. As previously mentioned, some operators are used just for the loser team and substitution strategy. On this basis, let set h, F, and S denote randomly selected position indexes, formation, and substitution property of the loser team, respectively. Subsequently, these property values of all players of set h are swapped together. The specific operator, named the winner strategy, is given, which is similar to those used in many evolutionary methods, such as PSO, to reach this goal in the proposed algorithm [8]. In this operator, first, we determine the position of the winning team and combine it with a random one to obtain a new position using the following formulas:

$$X^f(t+1) = X^f(t) + r_1\psi^f\left(X^f(t)^* - X^f(t)\right), \tag{26}$$

$$X^s(t+1) = X^s(t) + r_2\psi^s\left(X^s(t)^* - X^s(t)\right), \tag{27}$$

Where ψ^f and ψ^s symbolize inertia weights of formation and substitute properties, respectively, and r_1 and r_2 are random numbers, which are generated uniformly in [0, 1]. In the learning operator, coaches examine the behavior of teams for obtaining the best results to enhance their teams' performance. Moreover, we define the formula to explain the learning phase as follows:

$$X_j^g(t+1)_\Phi = \left(X_j^g(t)\right)_\Phi - \theta\left(\left|\vartheta\left(X_j^g(t)\right)_\Phi - X_j^g(t)\right|\right), \tag{28}$$

where g signifies a set that compromise substitute and formation properties ($g = \{s,f\}$), and index Φ yields a value from one to three, which indicates the first, second, and third best solutions, also known as ranks 1, 2, and 3, respectively. $X_j^g(t+1)_\Phi$ shows the value of position j of property g with respect to the best solution Φ. $X_j^g(t)$ is the value of position j of the current iteration t. Finally, θ and ϑ are coefficient values, which are defined as follows:

$$\theta = dbr_1 - b, \tag{29}$$

$$\vartheta = dr_2, \tag{30}$$

Where r_1 and r_2 are random numbers that are uniformly generated between zero to one, and b is linearly decreased from β to zero, which is computed as follows:

$$b = \beta - (t(\beta/T)). \tag{31}$$

The coaches pursue to recognize the best combination of active (formation) and passive players (substitutes) concerning the top three teams in the league. Therefore, the following formulas are assumed to capture the learning phase for formation property:

$$X_j^f(t+1)_1 = \left(X_j^f(t)\right)_1 - \theta\left(\left|\vartheta\left(X_j^f(t)\right)_1 - X_j^f(t)\right|\right), \tag{32}$$

$$X_j^f(t+1)_2 = \left(X_j^f(t)\right)_2 - \theta\left(|\vartheta\left(X_j^f(t)\right)_2 - X_j^f(t)|\right), \tag{33}$$

$$X_j^f(t+1)_3 = \left(X_j^f(t)\right)_3 - \theta\left(|\vartheta\left(X_j^f(t)\right)_2 - X_j^f(t)|\right), \tag{34}$$

$$X_j^f(t+1) = \frac{X_j^f(t+1)_1 + X_j^f(t+1)_2 + X_j^f(t+1)_3}{3} \tag{35}$$

Similarly, the formulas mentioned above can also be used for substitute property by using term s instead of f in the corresponding position. Notably, we have used these formulas to enhance the exploitation process of the proposed algorithm. The transfer process takes place when a season ends. On this occasion, the players can move among teams. On this basis, we have mathematically expressed this concept in the proposed algorithm to perform the convergence toward an optimal solution.

Let set H be the randomly selected teams for this operator if only if a random value (r), generated randomly between 0 to 1, is greater than 0.5. Thus, the number of teams involved in the season transfer is expressed as follows:

$$N_{st} = [N\delta_{st}]. \tag{36}$$

where δ_{st} denotes the percentage of teams in this operator. Similar to the typical league in a volleyball game, top teams of any league go up to a higher division. Consequently, the worst teams are dropped down to the lower division. While only one league exists in this algorithm. The relegation of the worst teams is considered in this operator, which is called promotion and relegation. Thus, we intentionally eradicate the worst teams and then exchange them by new ones that are generated randomly. Let N_{pr} be the number of teams moving up to the upper league, and N be the total number of teams in the current league.

$$N_{pr} = \left[N\delta_{pr}\right], \tag{37}$$

where δ_{pr} symbolizes the percentage of teams, which are relegated and promoted accordingly.

3.4 Whale optimization algorithm

The WOA is presented in [30] as a new metaheuristic algorithm based on the social behavior of the humpback whales.

Moreover, the WOA begins by randomly generating a set of N solutions TH, which represents the solution for the given problem. Then, for each solution TH_i, $i = 1, 2, \ldots, N$, the objective function is computed, and the best solution is determined TH^*. Subsequently, each solution is updated either by using the encircling or bubble-net methods. In the bubble-net method, the current solution TH_i is updated using the shrinking encircling method, in which the value of a is decreased, as shown in the following equation:

$$a = a - a\frac{g}{g_{max}}. \tag{38}$$

where g and g_{max} are the current iteration and the maximum number of iterations, respectively.

Also, the solution TH_i can be updated using the encircling method, as shown in the following equation:

$$TH_i(g+1) = TH_i(g) - A\odot D, A = 2a\odot r_1 - a, \tag{39}$$

$$D = \left|C\odot TH^*(g) - TH_i(g)\right|, B = 2r_2, \tag{40}$$

where D is the distance between TH^* and TH_i at the gth iteration. The $r_1$and r_2 represent the random numbers, and the symbol ⊙ is the element-wise multiplication operation. Moreover, the value of a is decreased in the interval [2, 0] with increasing iterations using Eq. (38).

Also, the solution TH_i can be updated using the spiral method that simulates the helix-shaped movement around the TH^*, as shown in the following equation:

$$TH_i(g+1) = D^{'}\odot e^{bl}\odot\cos(2\pi l) + TH_i(g), D^{'} = \left|TH^*(g) - TH_i(g)\right|, \tag{41}$$

where $l \in [-1, 1]$ and b are the random variables and constant value used to determine the shape of a logarithmic spiral.

Moreover, the solutions in the WOA can be updated by using either the spiral-shaped path and shrinking, as defined in the following equation:

$$TH_i(g+1) = \begin{cases} TH^*(g) - A \odot D & if \quad r_3 \geq 0.5 \\ D^{'\odot e^{bl}} \odot \cos(2\pi l) + TH_i(g) & otherwise \end{cases} \tag{42}$$

where $r_3 \in [0, 1]$ represents the probability of switching between the spiral-shaped path and shrinking methods.

The whales can also search on the TH^* by using a random solution TH_r, as follows:

$$TH_i(g+1) = TH_r - A \odot D, \quad D^{'} = |TH_r(g) - TH_i(g)| \tag{43}$$

According to [30], the process of updating the solutions depends on a, A, C, and r_3. The current solution TH_i is updated using Eq. (41) when $r_3 \geq 0.5$; otherwise, it is updated using Eqs. (39)–(40) when $|A| < 1$ or Eq. (44) when $|A| \geq 1$. The process of updating the solutions is repeated until the stopping criteria are satisfied.

3.5 Proposed method

In this section, the main steps of the proposed VPLWOA for determining the optimal threshold values for image segmentation are discussed. The VPLWOA depends on improving the VPL algorithm using the operators of the WOA. Hence, the method is called VPLWOA. In the VPLWOA, the Otsu's function (as defined in Eq. (3)) is used to evaluate the quality of each solution.

The proposed approach begins by computing the histogram of the given image I, and then generates a random set of N teams (TH) as:

$$TH_{ij}^{f} = LH_j + rand \times \left(HH_j - LH_j\right), i = 1, 2, \ldots, N, j = 1, 2, \ldots, K, \tag{44}$$

$$TH_{ij}^{s} = LH_j + rand \times \left(HH_j - LH_j\right), i = 1, 2, \ldots, N, j = 1, 2, \ldots, K, \tag{45}$$

where LH_j and HH_j are the lower and higher histogram values at the jth dimension. The next step in the proposed VPLWOA approach is to create the league schedule and evaluate the quality of each team TH_i by computing the objective function (as defined in Eq. (2)). Then, the VPLWOA performs the competition between each team to determine the loser and winner teams using Eqs. (9)–(10). Knowledge sharing, repositioning, and substitution strategies are used to improve the behavior of the loser teams; whereas, the leading role strategy is applied for the winning teams. Thereafter, the behaviors of all competitive teams are enhanced during the modified learning phase (the main contribution). The VPLWOA can simultaneously update the behavior of the team by using the operators of the WOA and traditional learning phase, as shown in the following equation:

$$TH_i^f = \begin{cases} Traditional\ learning\ phase, & Prob_i > r_5 \\ Operators\ of\ WOA, & otherwise \end{cases}, \tag{46}$$

where $r_5 \in [0, 1]$ is a random number used to switching between the VPL and WOA. The $Prob_i$ represents the probability of the fitness function (f_i) for the ith team and is defined as follows:

$$Prob_i = \frac{f_i}{\sum_{i=1}^{n} f_i}. \tag{47}$$

The next step in the proposed VPLWOA is to use the promotion and relegation and season transfer processes similar to the traditional VPL. The previously mentioned steps are performed until the terminal criteria are satisfied. The full steps of the developed VLPWOA are given in Algorithm 1.

Algorithm 1: Pseudo-code of the VLPWOA approach

```
Input: maximum number of generations, parameters, and cost function
Output: the best solution
Initialization stage
$g = 1$
While $g < g_{max}$
    Generate a league schedule
    For i = 1: $(N - 1)×2$
        Best team = select the best team according to the cost functions
        Apply competition procedure between teams $A$ and $B$
        Determine the winner and loser teams
        Apply different strategies for the winner and loser teams
        For j = 1: number of teams
            Compute $Prob_j$ using Eq.(48).
            If $Prob_j \geq r_5$
                Update the position of the team($j$) by using VPL
            Else
                Update the position of the team($j$) by using WOA
            End if
        End for
    End for
    Apply promotion and relegation process
    Apply season transfer process
    $g = g + 1$
End while
```

4 Experiments and discussion

In this section, a set of experimental series is performed to verify the performance of the proposed VPLWOA method. Two different sets of images are also used, and the results of VPLWOA are compared with other methods. The parameter setting and performance measure to evaluate the performance of the algorithms are discussed in this section. Then, experimental series one is performed using the first set of images that contains eleven images. Experimental series two is performed using the second set of images that have six medical graphics for leukemia blood cells.

4.1 Parameter setting

The results of the proposed VPLWOA are compared with the other five methods. These methods are social-spider optimization [37], sine–cosine algorithm [35], FA [21], WOA [9], and traditional VPL [32]. These approaches are selected because their performance is established in several fields, including image segmentation. However, the VPL is used for the first time in image segmentation.

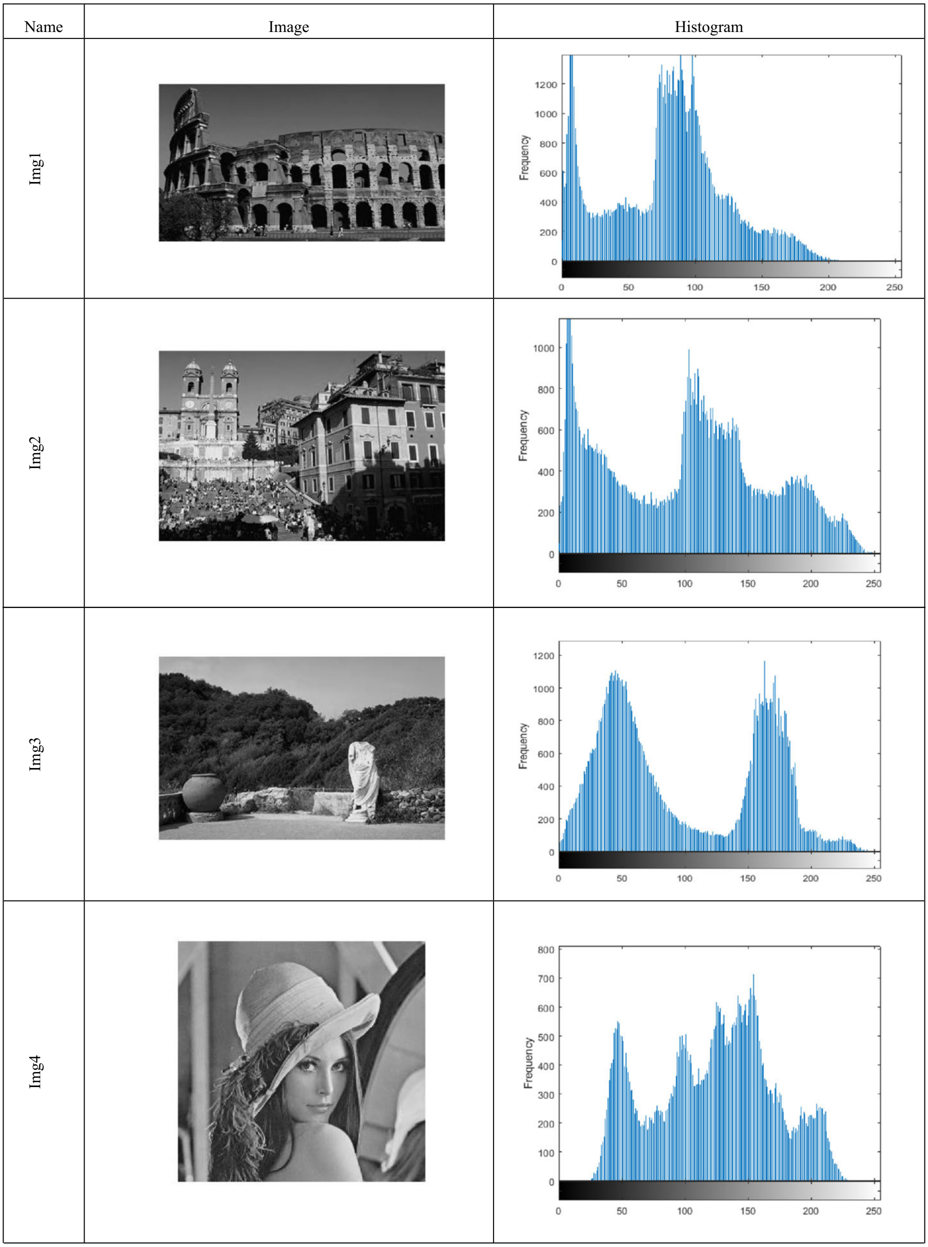

Fig. 2 Original images and their histogram

Img5	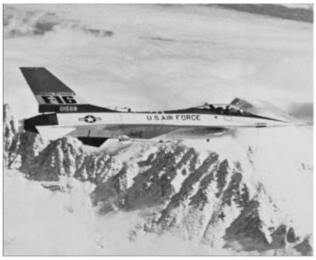	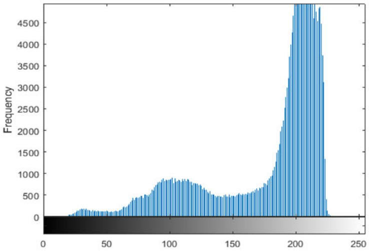
Img6	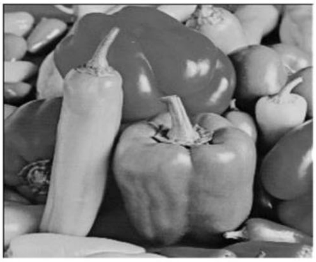	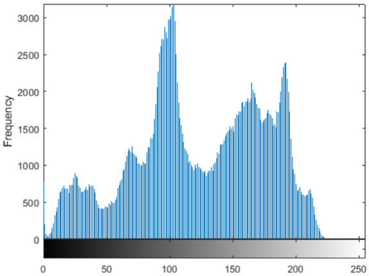
Img7	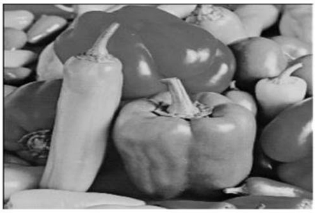	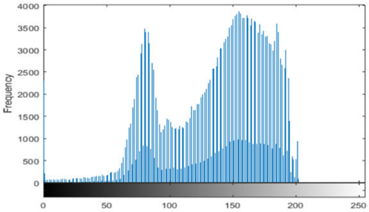
Img8	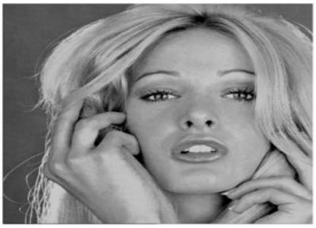	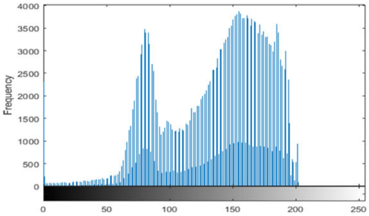

Fig. 2 (continued)

The value of the parameters for each algorithm is set similar to the original reference. The size of the population and the maximum number of iterations are set at 25 and 100, respectively. Each algorithm was executed 25 independent times along with each threshold level overall the tested images. A total of eight different levels of the threshold are used to segment each image to two, four, six, eight, 10, 16, 18, and 20. All the algorithms are implemented using MATLAB 2017b, which is installed in Windows 10 (64 bits).

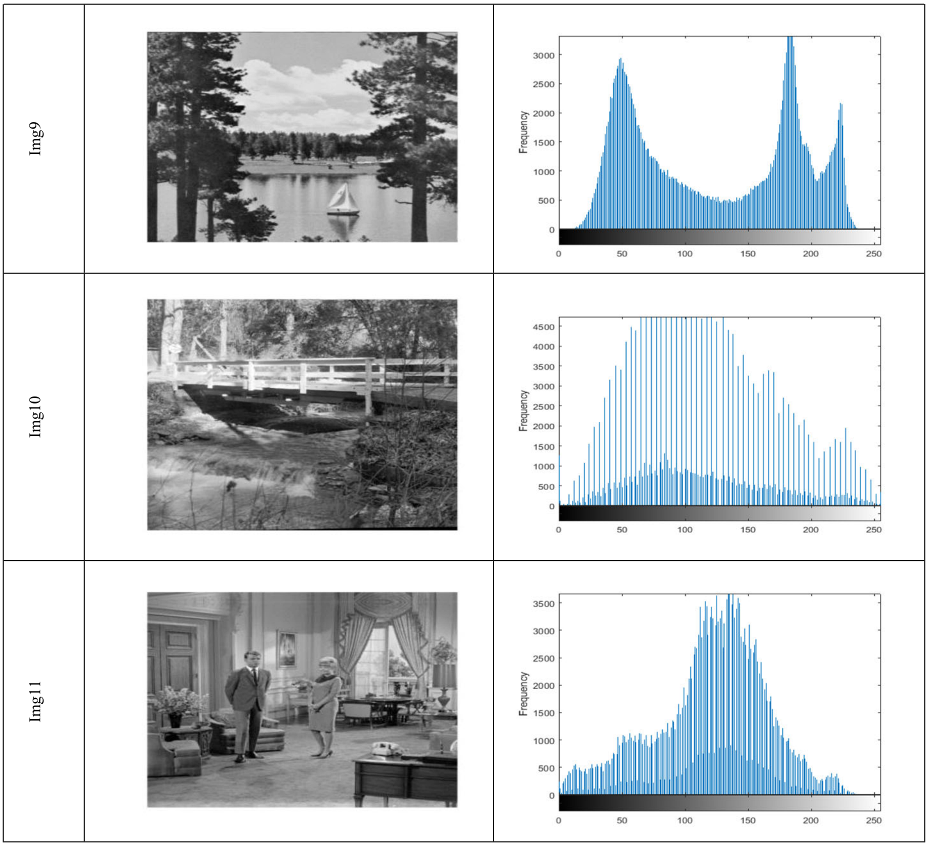

Fig. 2 (continued)

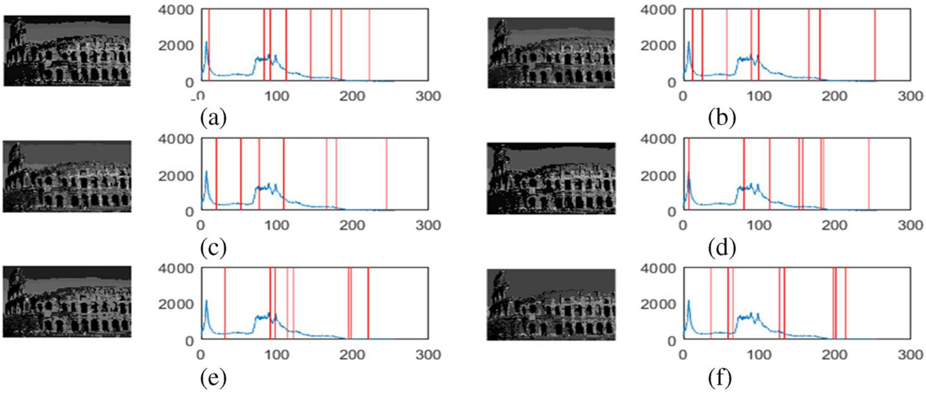

Fig. 3 Results of histogram and corresponding thresholds over a segmented image at threshold eight. **a** FA, **b** SCA, **c** SSO, **d** VPL, **e** WOA, **f** VPLWOA

Table 1 Results of the PSNR measurement

Thresholds	Image	FA	SCA	SSO	VPL	WOA	VPLWOA
2	Img1	16.9862	16.8935	17.1603	17.3468	17.1875	17.0841
	Img2	13.2816	13.6248	13.3721	13.4621	13.7191	13.6955
	Img3	14.7014	14.6223	14.6354	14.5269	14.8620	14.5815
	Img4	15.4938	15.5432	15.0432	15.2320	15.2529	15.2961
	Img5	14.8236	14.2742	14.2438	14.5781	14.5772	14.4622
	Img6	10.8031	10.3949	10.2884	10.6508	10.7562	10.9401
	Img7	14.1213	14.2473	14.4905	14.0071	14.4507	14.2719
	Img8	13.3395	12.6509	12.8209	13.0921	12.6868	13.0681
	Img9	15.0914	14.9508	15.1863	14.8873	14.7754	15.5376
	Img10	14.0840	13.9958	13.7820	13.7806	14.0249	14.2581
	Img11	14.5445	14.8750	14.5309	14.8307	14.5633	14.0745
4	Img1	19.6342	19.7965	19.9100	19.9361	19.9437	20.2089
	Img2	16.3032	16.3605	15.9675	16.8962	16.5774	16.7006
	Img3	18.6885	17.7943	18.2413	17.8756	18.0391	17.5693
	Img4	17.9319	18.3011	18.2807	17.8867	17.6242	18.4572
	Img5	17.6923	17.4820	17.9605	18.2067	17.9319	17.8631
	Img6	13.6680	15.0067	13.9716	13.2850	13.5077	15.0171
	Img7	17.5034	17.3859	17.8057	17.9000	17.8836	17.0503
	Img8	16.1245	16.5052	15.7997	15.3265	15.3318	16.6781
	Img9	18.7365	18.2300	18.7015	18.5667	18.4587	18.6853
	Img10	17.4172	17.1563	17.2624	17.2452	17.4938	17.0338
	Img11	17.7822	17.9915	18.3657	18.2104	18.0186	17.9002
6	Img1	21.8711	22.1926	22.3355	22.0531	21.7297	22.2850
	Img2	19.0305	19.5836	18.3253	19.0123	19.4015	19.2176
	Img3	19.7792	19.9261	19.9955	20.1673	20.2162	19.4665
	Img4	20.4034	20.3900	20.2203	20.5867	20.4517	20.1880
	Img5	20.3119	19.8147	19.5662	19.9159	19.7799	20.1632
	Img6	16.6484	18.0173	17.5689	16.3299	15.5464	16.7274
	Img7	19.3891	19.7564	19.1947	19.7649	19.4240	20.0239
	Img8	18.1171	18.1848	18.4227	17.5898	17.8169	18.1277
	Img9	20.5292	20.2279	20.4146	20.2544	20.7545	20.4219
	Img10	19.0979	19.5323	19.5047	19.7654	19.4606	19.7980
	Img11	20.5565	19.9965	19.6923	20.9513	20.1597	20.0072
8	Img1	23.4005	23.6178	23.4981	23.2342	23.8442	24.0403
	Img2	21.0204	20.3202	20.4069	20.9336	20.8015	21.1191
	Img3	21.5551	21.6998	21.6198	21.8398	21.1747	22.0062
	Img4	21.8089	21.6952	21.8598	21.5358	21.6700	22.2265
	Img5	21.7953	21.6565	21.4703	21.5033	21.6945	21.6175
	Img6	18.9127	18.9125	18.1487	18.3825	19.7630	18.5474
	Img7	20.8264	21.8325	21.3857	21.5586	21.5723	21.1429
	Img8	19.8939	20.4165	19.7376	20.8707	20.1677	19.8744
	Img9	21.9230	21.6003	21.7185	22.1995	21.9198	21.9226
	Img10	20.6575	20.7922	21.1773	20.8688	21.1152	21.0868
	Img11	22.4731	21.5464	21.9168	21.8332	21.2763	21.3172
10	Img1	24.9131	24.6436	25.1112	25.1223	24.7852	25.2767
	Img2	22.9298	22.3258	22.2202	21.6003	21.8324	21.8329
	Img3	22.8483	22.7410	22.8056	22.8915	23.0721	23.2224
	Img4	22.8853	22.2719	23.0292	22.6176	23.0109	22.5664
	Img5	22.5748	22.7365	22.7957	22.7754	22.6471	23.0254
	Img6	20.4181	20.7873	21.6068	21.0494	20.3512	20.4688
	Img7	22.4259	23.2611	22.9225	22.9851	23.0355	22.8292
	Img8	21.5567	20.9912	21.7195	21.7886	21.8700	21.7690
	Img9	22.9021	23.1008	23.3730	23.1387	23.4843	23.2412
	Img10	22.7883	22.8892	22.4168	22.5975	22.3539	22.4242
	Img11	23.3315	22.7852	22.9233	23.4181	22.4418	23.3100
16	Img1	27.6762	27.2667	27.5283	27.3741	27.5076	27.0934

Table 1 (continued)

Thresholds	Image	FA	SCA	SSO	VPL	WOA	VPLWOA
	Img2	25.0974	25.2490	25.2954	24.5264	25.2225	24.9576
	Img3	26.2217	26.1339	26.3436	26.1970	26.2373	25.9069
	Img4	25.7223	25.8743	25.8358	26.5395	25.9065	25.7018
	Img5	25.8069	25.4509	25.6042	25.8854	26.1860	25.7348
	Img6	24.0556	24.5077	24.1605	24.6704	22.5051	24.1373
	Img7	25.8530	25.8553	25.6168	25.7108	26.1082	26.2627
	Img8	25.3821	24.9393	24.5859	25.3535	25.1894	24.6683
	Img9	26.0149	25.6271	25.7360	26.3322	26.0496	26.5161
	Img10	25.8328	26.0055	25.7168	25.5605	25.6689	25.4011
	Img11	25.8789	25.9319	25.7039	25.7906	26.5908	26.2482
18	Img1	27.7591	27.9813	27.8874	27.8711	28.5719	27.9615
	Img2	26.3565	26.3264	26.6271	25.8362	25.8313	25.3133
	Img3	26.6226	26.7536	27.2143	26.6853	26.3976	26.8314
	Img4	26.9177	25.9322	26.5718	26.4380	26.3406	26.9832
	Img5	26.2371	26.1858	26.9611	26.5100	26.5049	26.2094
	Img6	24.5866	24.4716	23.8208	24.5621	24.3140	24.9845
	Img7	27.0527	25.9377	26.7618	26.9897	26.5329	26.1927
	Img8	25.9400	25.7817	25.5159	25.4062	26.4015	25.6718
	Img9	26.7999	26.5582	26.9210	26.5695	26.1238	26.9544
	Img10	26.1791	26.0432	26.3823	25.9803	26.1400	26.4556
	Img11	27.0401	26.8415	26.7430	26.0961	27.0144	26.9094
20	Img1	28.8200	28.2206	28.9546	28.4840	28.9119	28.2841
	Img2	26.9989	26.5946	27.0054	27.3749	27.3322	26.5047
	Img3	27.1811	27.3694	27.9064	26.9528	26.7792	27.0252
	Img4	27.0817	26.2157	26.9658	26.4252	27.2940	27.4291
	Img5	26.9088	27.5567	27.3600	27.5012	26.7439	26.7573
	Img6	25.7701	24.9364	26.2360	25.9663	26.2371	25.2798
	Img7	27.1759	26.8212	27.8297	26.7927	27.0538	27.6239
	Img8	27.1320	27.3327	26.5732	26.3279	26.3411	25.5980
	Img9	27.5672	27.4286	27.8230	27.2482	27.7252	27.8239
	Img10	26.9166	26.8282	26.9848	27.0354	27.0661	27.2370
	Img11	27.3730	27.5262	26.8973	26.9435	27.0785	27.9653
Mean		21.8442	21.7820	21.8295	21.8046	21.7977	21.8449

4.2 Performance measures

A set of three performance measures are used to verify the performance of proposed VPLWOA, including peak signal-to-noise ratio (PSNR) Eq.(48), structural similarity index (SSIM) Eq. (50), fitness value (Otsu's method is used as a fitness function), and CPU time. All results are tabulated and summarized in figures.

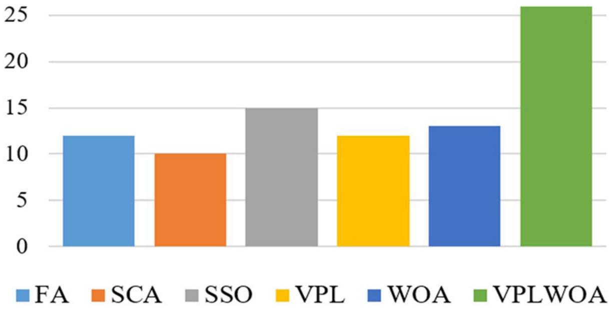

Fig. 4 PSNR ranking of all algorithms

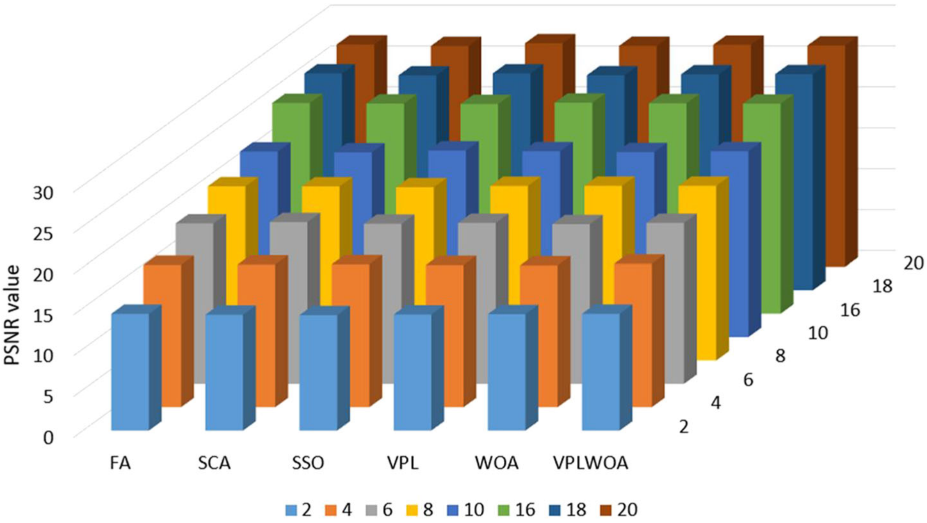

Fig. 5 Average of the PSNR for all algorithms at each threshold level

Table 2 Results of SSIM measurement

Thresholds	Image	FA	SCA	SSO	VPL	WOA	VPLWOA
2	Img1	0.62007	0.63155	0.62947	0.64640	0.63715	0.63186
	Img2	0.55168	0.55300	0.54803	0.55257	0.56523	0.55384
	Img3	0.54377	0.53753	0.54016	0.53564	0.54395	0.53245
	Img4	0.52383	0.54937	0.52714	0.53655	0.54037	0.52874
	Img5	0.59020	0.56884	0.57902	0.57992	0.58575	0.57883
	Img6	0.64846	0.63458	0.62959	0.64663	0.64851	0.65495
	Img7	0.60689	0.60665	0.61443	0.60847	0.61138	0.61210
	Img8	0.56698	0.54439	0.55416	0.54765	0.54701	0.55928
	Img9	0.52741	0.52098	0.53480	0.52159	0.52232	0.54442
	Img10	0.51784	0.51099	0.50089	0.51950	0.51008	0.50525
	Img11	0.58516	0.59776	0.58666	0.58575	0.59709	0.58516
4	Img1	0.75152	0.73157	0.73265	0.74466	0.73718	0.73101
	Img2	0.70734	0.69656	0.67500	0.69769	0.70686	0.68571
	Img3	0.68303	0.66521	0.67242	0.66969	0.68518	0.66582
	Img4	0.66515	0.67008	0.66349	0.64503	0.65041	0.67427
	Img5	0.68432	0.69230	0.69433	0.70338	0.69295	0.70058
	Img6	0.72783	0.76940	0.74140	0.72477	0.71779	0.75041
	Img7	0.69644	0.69312	0.69607	0.68898	0.69318	0.69664
	Img8	0.68544	0.66179	0.67548	0.67163	0.67151	0.68019
	Img9	0.66903	0.65581	0.66893	0.66342	0.66159	0.66908
	Img10	0.67230	0.66341	0.67123	0.67060	0.67279	0.66705
	Img11	0.67324	0.67231	0.68064	0.68115	0.67647	0.66814
6	Img1	0.79139	0.80993	0.79955	0.80387	0.79338	0.79875
	Img2	0.78000	0.78954	0.79261	0.78299	0.78469	0.78459
	Img3	0.74271	0.74306	0.75043	0.75201	0.73621	0.72995
	Img4	0.76452	0.74915	0.74879	0.73331	0.74042	0.73414
	Img5	0.75337	0.74868	0.74835	0.75195	0.74770	0.75856
	Img6	0.78010	0.79715	0.78944	0.77581	0.75769	0.78408
	Img7	0.73565	0.74193	0.73885	0.73971	0.73636	0.73717
	Img8	0.74491	0.72207	0.72770	0.72875	0.73023	0.74149
	Img9	0.72997	0.71769	0.72779	0.72180	0.73227	0.72590
	Img10	0.74584	0.75258	0.75511	0.75461	0.75412	0.76505

Table 2 (continued)

Thresholds	Image	FA	SCA	SSO	VPL	WOA	VPLWOA
	Img11	0.72512	0.71959	0.71829	0.73485	0.72624	0.72201
8	Img1	0.83465	0.83274	0.82936	0.82961	0.83625	0.83236
	Img2	0.83022	0.81869	0.83049	0.83798	0.82977	0.83588
	Img3	0.78725	0.79040	0.79685	0.79661	0.78906	0.80267
	Img4	0.79390	0.79712	0.79315	0.78668	0.77327	0.79252
	Img5	0.78530	0.78842	0.78941	0.78515	0.79004	0.79062
	Img6	0.79754	0.79183	0.77495	0.79418	0.81333	0.80073
	Img7	0.76955	0.76395	0.76719	0.76216	0.77385	0.76990
	Img8	0.78343	0.78284	0.76606	0.78341	0.76120	0.76736
	Img9	0.76176	0.75645	0.76541	0.77553	0.76999	0.76295
	Img10	0.79469	0.79342	0.80503	0.80223	0.79821	0.80305
	Img11	0.76679	0.75258	0.75893	0.75663	0.75419	0.76395
10	Img1	0.85393	0.85126	0.86114	0.85099	0.85786	0.85692
	Img2	0.86085	0.85327	0.86212	0.86015	0.86448	0.84318
	Img3	0.82542	0.80763	0.81514	0.82625	0.81150	0.81515
	Img4	0.81674	0.81181	0.80371	0.80668	0.81400	0.80677
	Img5	0.81139	0.81460	0.81419	0.80777	0.80816	0.80845
	Img6	0.83596	0.82182	0.83152	0.82765	0.83215	0.83299
	Img7	0.78608	0.79426	0.78940	0.79323	0.79614	0.81313
	Img8	0.79260	0.77799	0.80316	0.81062	0.81100	0.80267
	Img9	0.78946	0.79534	0.80092	0.79660	0.80563	0.79799
	Img10	0.83321	0.84227	0.83723	0.83698	0.83503	0.84430
	Img11	0.78419	0.77809	0.77896	0.78340	0.77011	0.78662
16	Img1	0.90309	0.89723	0.89111	0.90074	0.89362	0.89316
	Img2	0.90714	0.90743	0.90890	0.88984	0.91142	0.90814
	Img3	0.89022	0.87489	0.88257	0.87913	0.87152	0.88039
	Img4	0.87810	0.88037	0.87324	0.88613	0.87160	0.87360
	Img5	0.86509	0.85639	0.86148	0.86612	0.86943	0.86321
	Img6	0.85456	0.85087	0.85834	0.86093	0.84822	0.85379
	Img7	0.84555	0.84044	0.84054	0.84534	0.84466	0.84682
	Img8	0.85458	0.85425	0.85009	0.84894	0.85948	0.86234
	Img9	0.85912	0.84753	0.86324	0.86138	0.85539	0.84868
	Img10	0.89768	0.89241	0.89531	0.89361	0.89658	0.89853
	Img11	0.83583	0.83681	0.83795	0.83971	0.84713	0.84060
18	Img1	0.89989	0.90440	0.90409	0.90427	0.90525	0.89976
	Img2	0.91568	0.91765	0.92067	0.91541	0.91283	0.92272
	Img3	0.88911	0.89435	0.89316	0.88739	0.88993	0.88571
	Img4	0.88548	0.87562	0.87823	0.88102	0.88474	0.89268
	Img5	0.87071	0.87146	0.88009	0.86997	0.87076	0.87427
	Img6	0.85141	0.85844	0.86367	0.86135	0.86176	0.88035
	Img7	0.86011	0.84889	0.85520	0.85587	0.85473	0.85340
	Img8	0.86045	0.86248	0.86570	0.86360	0.86810	0.86159
	Img9	0.86652	0.86377	0.87029	0.86366	0.85799	0.87157
	Img10	0.90457	0.90303	0.90631	0.90356	0.89989	0.90686
	Img11	0.85625	0.85331	0.84847	0.84114	0.85254	0.84888
20	Img1	0.91490	0.90339	0.91016	0.91534	0.90493	0.90802
	Img2	0.92091	0.91383	0.93098	0.92135	0.93193	0.92561
	Img3	0.89921	0.91193	0.90325	0.88678	0.89498	0.88790
	Img4	0.89685	0.88324	0.89057	0.88823	0.89949	0.89371
	Img5	0.87979	0.88946	0.88626	0.88296	0.87717	0.87991
	Img6	0.88307	0.86524	0.87218	0.86817	0.87648	0.86861
	Img7	0.86612	0.85758	0.86956	0.85634	0.86260	0.87039
	Img8	0.88052	0.88322	0.87936	0.87173	0.87383	0.87501
	Img9	0.88274	0.87620	0.88605	0.87728	0.88568	0.88642
	Img10	0.91520	0.91304	0.91879	0.91296	0.91590	0.91466
	Img11	0.86196	0.86802	0.84826	0.85719	0.85733	0.87540
Mean		0.78340	0.78060	0.78217	0.78170	0.78201	0.78341

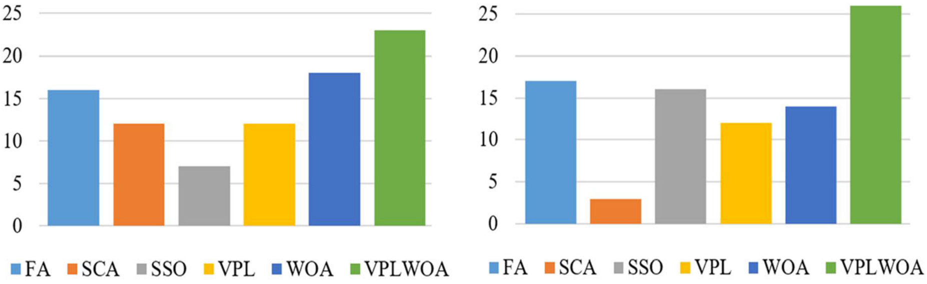

(a) (b)

Fig. 6 **a** SSIM ranking of all algorithms. **b** Ranking of the fitness values

$$PSNR = 20Log_{10}\left(\frac{255}{RMSE}\right), \tag{48}$$

$$RMSE = \sqrt{\frac{\sum_{i=1}^{M}\sum_{j=1}^{Q}\left(I(i,j) - I_s(i,j)\right)^2}{M \times Q}} \tag{49}$$

$$SSIM(I, I_s) = \frac{\left(2\mu_I\mu_{I_s} + c_1\right)\left(2\sigma_{I,I_s} + c_2\right)}{\left(\mu_I^2 + \pi_{I_s}^2 + c_1\right)\left(\sigma_I^1 + \sigma_{I_s}^2 + c_2\right)}, \tag{50}$$

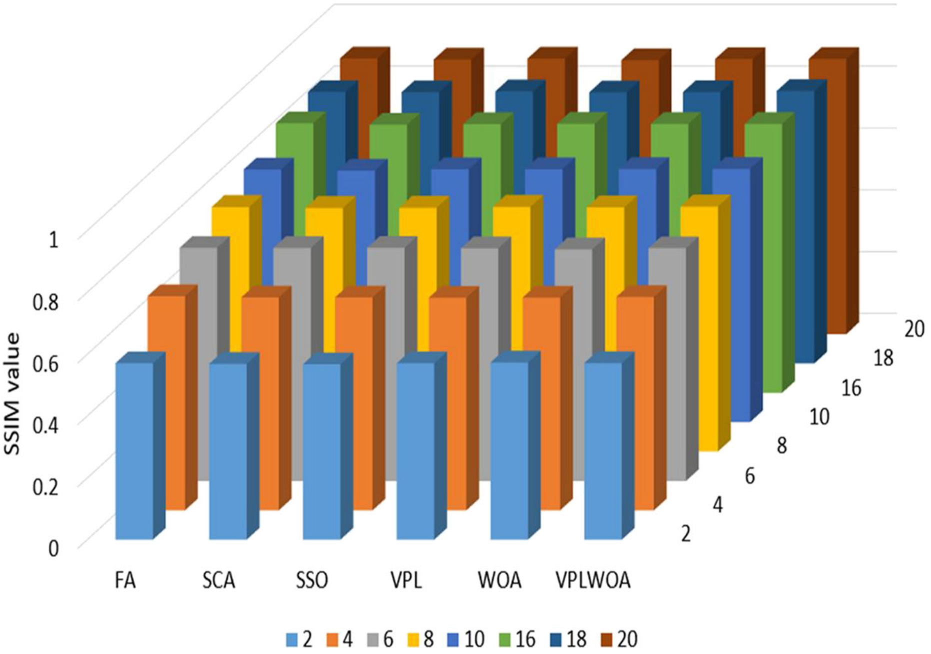

Fig. 7 Average of the SSIM for all algorithms at each threshold level

Table 3 Results of the fitness value for all algorithms

Thresholds	Image	FA	SCA	SSO	VPL	WOA	VPLWOA
2	Img1	1703.456	1712.468	1711.894	1734.926	1725.392	1713.615
	Img2	1708.328	1687.862	1725.929	1711.276	1729.670	1713.464
	Img3	1724.513	1694.385	1713.239	1708.673	1733.949	1736.985
	Img4	1724.520	1726.138	1714.449	1701.156	1698.402	1722.211
	Img5	4991.201	4950.548	4962.917	4983.714	5001.077	4984.048
	Img6	1581.792	1587.016	1588.829	1586.535	1585.781	1584.810
	Img7	1581.144	1582.674	1585.659	1584.588	1583.912	1590.158
	Img8	1589.786	1579.850	1580.631	1583.905	1585.623	1589.878
	Img9	1584.106	1583.971	1586.660	1593.023	1583.499	1584.887
	Img10	1588.729	1583.783	1585.024	1590.103	1582.797	1585.010
	Img11	1579.357	1584.041	1578.944	1576.600	1588.166	1580.550
4	Img1	1880.266	1875.024	1863.270	1873.830	1878.473	1864.501
	Img2	1883.126	1873.014	1872.826	1878.365	1878.864	1873.284
	Img3	1891.211	1865.781	1881.080	1870.542	1875.042	1872.578
	Img4	1874.896	1875.750	1869.678	1875.425	1879.000	1881.252
	Img5	5216.947	5218.272	5224.690	5233.415	5222.599	5238.445
	Img6	1646.383	1648.282	1649.349	1645.340	1641.283	1649.298
	Img7	1642.318	1645.523	1646.438	1643.822	1647.067	1647.473
	Img8	1645.481	1643.398	1646.144	1644.864	1644.308	1651.244
	Img9	1645.896	1642.698	1649.793	1648.858	1647.242	1650.972
	Img10	1645.121	1639.877	1646.028	1644.678	1645.269	1648.037
	Img11	1646.481	1646.782	1639.757	1648.802	1644.731	1646.305
6	Img1	1936.724	1943.265	1946.757	1935.825	1932.088	1940.910
	Img2	1937.723	1940.812	1933.451	1934.636	1937.021	1942.985
	Img3	1939.130	1940.977	1943.996	1944.390	1938.656	1944.699
	Img4	1949.749	1938.982	1942.062	1939.091	1929.229	1933.273
	Img5	5320.981	5314.785	5324.966	5322.433	5314.672	5326.078
	Img6	1669.798	1667.301	1670.316	1668.778	1670.771	1671.528
	Img7	1670.176	1670.114	1668.018	1669.107	1667.986	1668.906
	Img8	1671.052	1667.890	1665.367	1669.956	1668.178	1669.466
	Img9	1670.098	1668.495	1671.635	1667.210	1670.245	1669.733
	Img10	1667.459	1668.249	1670.933	1671.194	1670.717	1672.183
	Img11	1669.845	1666.510	1668.733	1670.057	1670.452	1669.176
8	Img1	1969.910	1969.996	1971.522	1965.633	1971.525	1979.465
	Img2	1969.583	1969.388	1977.017	1977.974	1976.591	1967.421
	Img3	1979.697	1973.113	1965.554	1978.375	1966.828	1976.470
	Img4	1977.538	1969.431	1974.153	1970.882	1967.643	1973.971
	Img5	5372.387	5368.011	5368.828	5362.795	5369.879	5373.830
	Img6	1681.891	1682.540	1681.386	1681.988	1682.062	1681.316
	Img7	1681.365	1679.654	1681.552	1680.014	1683.024	1680.958
	Img8	1682.874	1681.450	1681.727	1681.702	1680.891	1680.439
	Img9	1680.004	1678.793	1681.110	1683.465	1681.823	1682.041
	Img10	1682.271	1678.720	1682.618	1682.315	1680.996	1682.159
	Img11	1682.297	1682.160	1681.707	1680.938	1682.940	1680.916
10	Img1	1990.431	1988.302	1992.985	1992.739	1988.937	1995.718
	Img2	1989.846	1989.727	1991.627	1987.391	1993.901	1987.550
	Img3	1991.617	1982.272	1989.948	1991.725	1987.954	1983.224
	Img4	1992.034	1990.704	1987.544	1991.167	1989.722	1991.375
	Img5	5394.623	5392.315	5399.817	5392.619	5392.841	5397.687
	Img6	1689.660	1688.722	1689.179	1689.525	1689.656	1689.690
	Img7	1686.208	1688.681	1688.886	1688.607	1689.402	1689.058
	Img8	1690.424	1685.208	1688.664	1688.127	1689.522	1687.526
	Img9	1687.180	1688.590	1687.812	1687.531	1689.867	1687.390
	Img10	1690.395	1688.587	1688.781	1688.665	1688.690	1688.352
	Img11	1687.900	1687.781	1689.748	1688.661	1687.864	1688.373
16	Img1	2016.800	2013.430	2017.447	2017.023	2016.951	2015.364

Table 3 (continued)

Thresholds	Image	FA	SCA	SSO	VPL	WOA	VPLWOA
	Img2	2016.590	2015.907	2016.962	2012.270	2018.092	2017.226
	Img3	2018.654	2018.339	2018.765	2019.093	2017.148	2017.648
	Img4	2018.135	2016.896	2016.444	2018.430	2017.962	2015.885
	Img5	5438.271	5433.432	5437.368	5437.218	5438.574	5437.083
	Img6	1697.317	1696.644	1698.112	1697.936	1697.921	1698.410
	Img7	1698.651	1698.606	1698.342	1698.515	1698.717	1698.737
	Img8	1698.501	1697.873	1698.916	1698.827	1697.757	1697.058
	Img9	1698.529	1696.035	1698.576	1698.087	1697.421	1697.605
	Img10	1698.305	1698.054	1697.960	1697.835	1698.562	1698.233
	Img11	1697.598	1697.661	1698.475	1699.315	1698.596	1697.381
18	Img1	2018.848	2020.102	2020.419	2019.776	2023.681	2020.558
	Img2	2021.382	2020.628	2022.967	2020.404	2018.636	2022.772
	Img3	2021.335	2021.488	2022.468	2020.472	2021.385	2019.220
	Img4	2021.508	2018.974	2020.616	2020.838	2021.338	2022.868
	Img5	5439.587	5442.411	5445.801	5439.403	5444.172	5441.609
	Img6	1700.246	1699.000	1699.802	1698.880	1700.041	1700.336
	Img7	1700.496	1699.619	1699.874	1699.989	1700.016	1699.656
	Img8	1699.626	1698.794	1699.347	1699.707	1700.438	1699.196
	Img9	1699.056	1699.161	1700.094	1699.321	1700.025	1698.867
	Img10	1700.230	1700.155	1699.514	1699.738	1699.900	1698.842
	Img11	1700.575	1699.832	1699.939	1699.511	1700.258	1699.678
20	Img1	2024.802	2022.751	2023.736	2023.926	2024.863	2026.248
	Img2	2024.885	2021.444	2025.606	2025.655	2025.529	2022.107
	Img3	2024.421	2020.847	2020.286	2022.098	2021.090	2026.276
	Img4	2025.917	2020.931	2024.377	2021.573	2022.553	2024.495
	Img5	5447.912	5447.243	5445.748	5448.770	5445.784	5442.893
	Img6	1701.980	1700.648	1700.412	1700.950	1701.446	1700.980
	Img7	1701.476	1700.213	1701.468	1701.583	1700.594	1701.904
	Img8	1700.864	1701.527	1701.106	1701.463	1701.016	1700.868
	Img9	1701.278	1701.106	1701.605	1700.433	1701.487	1701.386
	Img10	1700.953	1701.042	1701.736	1700.214	1700.238	1700.895
	Img11	1700.270	1701.583	1701.006	1701.040	1701.172	1701.721
Mean		2103.442	2100.921	2102.806	2102.821	2103.160	2103.714

where I and I_s are the original and segmented images, respectively; μ_I and μ_{I_s} are the mean intensities; σ_I^1 and $\sigma_{I_s}^2$ determine the standard deviation; σ is the covariance; $c_1 = 6.502$; and $c_2 = 58.522$.

4.3 Experimental series 1: benchmark images

In this experimental series, a set of eleven benchmark images are used to evaluate the accuracy of the VPLWOA to determine the optimal threshold values. These images have different properties, such as variant size, and resolutions. The histogram for the tested images is given in Fig. 2.

The comparison results of the VPLWOA with the other five methods are given in Figs. 5, 6, 7, 8 and 9 and Table 2 and For further analysis, the CPU time results for each algorithm are recorded in Table 3. From this table, the VPLWOA achieved the best results in 21 cases and is ranked third after both WOA (with 27 cases) and SSO (with 24 cases). The SCA obtained the fourth rank (with 10 cases) followed by the FA (with 6 cases), it was ranked fifth. Whereas, the VPL was considered as the slowest algorithm in the experiments. The VPLWOA showed good CPU time in a large threshold than the smallest one.

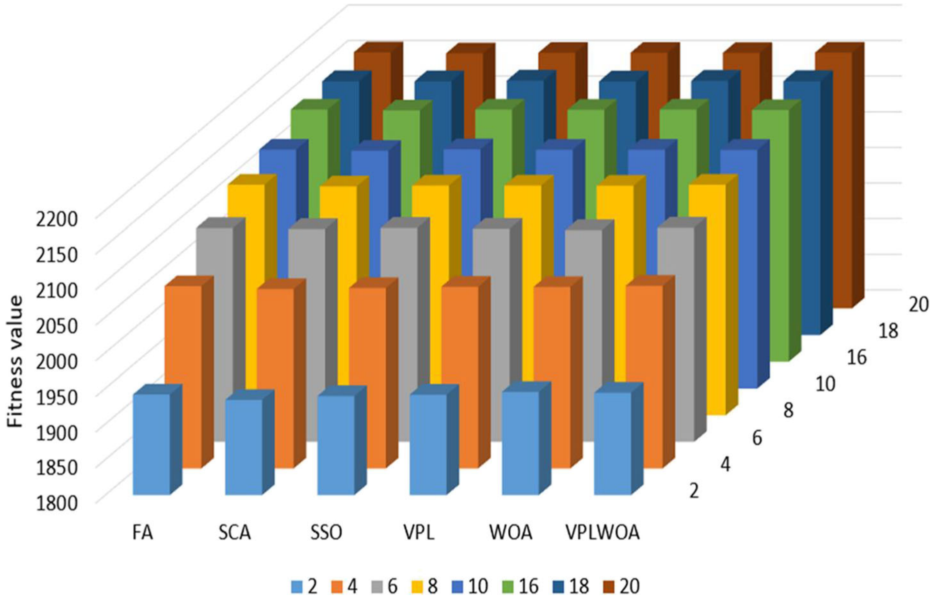

Fig. 8 Average of the fitness values for all algorithms at each threshold level

Table 4 whereas, Fig. 3 shows a sample of a segmented image and its histogram with the corresponding thresholds at level 8. The results of the PSNR measurement are listed in Table 1 and Fig. 4. As shown in this table, VPLWOA has achieved the best results in 26 cases out of 88 (11 images × eight thresholds), followed by SSO (with 15 cases), WOA (13 cases), VPL (12 cases), FA (12 cases), and SCA (10 cases). Moreover, the VPLWOA has obtained the best PSNR values in most images in six thresholds out of eight (i.e., two, four, eight, 10, 18, and 20); whereas, in thresholds six and 16, it performed equally with SSO, VPL, and WOA. In addition, Fig. 4 illustrates the PSNR ranking of the algorithms overall thresholds and images. The proposed VPLWOA method is better than the other algorithms, whereas Fig. 5 shows the average of the PSNR values for all algorithms at each threshold level.

The results of the SSIM measurement are shown in Table 2 and Fig. 6 (a). As shown in the table, VPLWOA has achieved the best results in 23 cases out of 88 (11 images × 8 thresholds), followed by WOA (with 18 cases), FA (with 16 cases), SCA (with 12 cases), VPL (with 12 cases), and SSO (with seven cases). Besides, the VPLWOA has obtained the best SSIM values in most images in threshold 18 and performed equally with WOA in thresholds 10 and 16. At threshold 2, all algorithms obtained the best SSIM value in two images except for SSO. The VPLWOA and FA outperformed all other algorithms in three images for each one in thresholds four and 20. However, the best algorithms are SCA and WOA at thresholds six and eight, respectively, followed by VPLWOA, VPL, and FA. Moreover, Fig. 8(a) illustrates the SSIM ranking of the algorithms overall thresholds and images. This approach achieved better results than other algorithms, whereas, Fig. 7 shows the average of the SSIM values for all algorithms at each threshold level.

The results of the fitness value are illustrated in Table 3. As shown in the table, VPLWOA has achieved the highest fitness value in 26 cases out of 88 (11 images × eight thresholds),

Table 4 CPU time was obtained by each algorithm

Thresholds	Image	FA	SCA	SSO	VPL	WOA	VPLWOA
2	Img1	0.2022	0.2045	0.2103	0.6251	0.1869	0.4105
	Img2	0.1953	0.2419	0.2003	0.5627	0.1760	0.4746
	Img3	0.3379	1.5403	1.1506	1.2506	0.3920	1.1734
	Img4	0.7806	0.7262	0.5917	0.7442	1.2155	0.6172
	Img5	0.3423	0.4351	0.2391	0.5371	0.3206	0.4052
	Img6	0.6497	0.3231	0.4015	0.5168	0.5045	0.3866
	Img7	0.4918	0.4501	0.3458	0.5368	1.9572	0.4037
	Img8	0.3049	0.3035	0.2941	0.5252	0.2966	0.3987
	Img9	0.3089	0.3075	0.2981	0.7579	0.2953	0.5518
	Img10	0.3028	0.3007	0.2942	0.5197	0.2919	0.3492
	Img11	0.3058	0.3033	0.2993	0.4999	0.2918	0.2857
4	Img1	0.2727	0.2420	0.2039	0.4771	0.2032	0.3827
	Img2	0.2036	0.2116	0.2131	0.6500	0.2158	0.4677
	Img3	0.2373	0.3730	0.2163	0.3901	0.2793	0.2640
	Img4	0.2873	1.5276	0.1734	0.4766	0.4261	0.3385
	Img5	1.5127	1.3529	0.9766	1.2575	0.8781	1.1817
	Img6	0.5174	0.5886	0.3999	0.6302	0.3849	0.4758
	Img7	2.2474	0.7447	0.6062	0.8582	0.6320	0.7324
	Img8	0.3343	0.3186	0.3128	0.7674	0.3111	0.5785
	Img9	0.3173	0.3211	0.3111	0.7156	0.3130	0.5263
	Img10	0.3259	0.3178	0.3150	0.7685	0.3034	0.6411
	Img11	0.3227	0.3180	0.3183	0.6012	0.3091	0.4933
6	Img1	0.3110	0.2132	0.2308	0.6504	0.2147	0.5290
	Img2	0.2337	0.2310	0.2399	0.3935	0.2197	0.1784
	Img3	0.3839	0.6003	0.3843	0.5104	0.6447	0.3684
	Img4	1.1227	0.3617	0.5346	0.7846	3.5723	0.6594
	Img5	0.9692	0.4990	0.3868	0.6362	0.6764	0.4515
	Img6	0.4025	0.3859	0.5560	0.8496	0.6305	0.7230
	Img7	0.6364	0.5864	0.3796	0.8673	0.3892	0.6623
	Img8	0.3332	0.3333	0.3292	0.5660	0.3234	0.4685
	Img9	0.3326	0.3353	0.3230	0.5240	0.3231	0.3988
	Img10	0.3335	0.3318	0.3231	0.6570	0.3466	0.4494
	Img11	0.3346	0.3372	0.3200	0.6295	0.3228	0.4821
8	Img1	0.2406	0.2516	0.2383	0.4037	0.2264	0.3201
	Img2	0.2300	0.2488	0.2319	0.5264	0.2267	0.3461
	Img3	0.5868	0.2019	0.2278	0.5262	0.5714	0.4555
	Img4	0.7221	1.6001	1.3738	1.8111	0.7654	1.2506
	Img5	0.8904	1.7213	1.1490	1.5715	0.6922	1.3579
	Img6	0.4337	0.8156	0.5367	0.9798	0.5664	0.8502
	Img7	0.8669	1.0865	0.4703	0.8142	0.8047	0.6345
	Img8	0.3413	0.3425	0.3333	0.6596	0.3398	0.4869
	Img9	0.3503	0.3473	0.3356	0.6804	0.3330	0.4636
	Img10	0.3441	0.3510	0.3420	0.4832	0.3337	0.3827
	Img11	0.3487	0.3514	0.3433	0.5066	0.3420	0.3476
10	Img1	0.2390	0.2426	0.2528	0.7334	0.2388	0.4602
	Img2	0.2675	0.2292	0.2513	0.4554	0.2355	0.1737
	Img3	0.5649	0.2682	0.4288	0.7347	0.8408	0.4058
	Img4	1.2186	1.5791	0.6133	0.9679	1.7173	0.6544
	Img5	0.3093	0.3412	0.2778	0.5382	0.4382	0.2222
	Img6	0.6658	0.5761	0.6460	0.9406	0.6861	0.6368
	Img7	0.5375	0.4684	0.4356	0.8357	1.6676	0.4938
	Img8	0.3611	0.3589	0.3502	0.5007	0.3500	0.1727
	Img9	0.3601	0.3655	0.3507	0.4679	0.3480	0.1852
	Img10	0.3610	0.3659	0.3545	0.6028	0.3559	0.2790
	Img11	0.3626	0.3627	0.3491	0.7264	0.3551	0.4327
16	Img1	0.3089	0.3109	0.2693	0.7436	0.2640	0.4344

Table 4 (continued)

Thresholds	Image	FA	SCA	SSO	VPL	WOA	VPLWOA
	Img2	0.3954	0.4252	0.3583	0.6493	0.3070	0.3879
	Img3	0.6055	1.0184	0.7830	0.9346	0.4263	0.6527
	Img4	1.5707	1.3989	2.7816	4.0752	2.5318	3.7630
	Img5	0.9095	0.5433	2.5066	1.9848	0.3279	1.6453
	Img6	1.1070	1.9950	0.6404	0.8875	2.3921	0.5411
	Img7	0.3927	0.4389	0.4030	0.6344	0.3918	0.3824
	Img8	0.3984	0.4155	0.3900	0.7991	0.3955	0.5381
	Img9	0.4024	0.4086	0.3970	0.6159	0.3927	0.3256
	Img10	0.3904	0.4331	0.3885	0.5596	0.3945	0.2999
	Img11	0.4108	0.4207	0.3908	0.7671	0.4042	0.4878
18	Img1	0.2957	0.3210	0.2701	0.4757	0.2695	0.1578
	Img2	0.2994	0.3032	0.2654	0.5485	0.2983	0.2006
	Img3	0.8833	0.6712	0.6500	1.0875	0.5037	0.7975
	Img4	1.7662	1.5250	2.8344	3.2870	0.9450	2.5549
	Img5	0.6127	4.5505	5.8708	6.2508	0.2685	4.9877
	Img6	0.9035	0.8290	0.7067	1.1090	1.3385	0.7745
	Img7	0.4038	0.4271	0.4048	0.8946	0.4105	0.6213
	Img8	0.4227	0.4343	0.4173	0.6782	0.4078	0.4214
	Img9	0.4103	0.4324	0.4062	0.5587	0.4072	0.2756
	Img10	0.4163	0.4385	0.3972	0.7871	0.4028	0.4796
	Img11	0.4225	0.4295	0.4045	0.8643	0.4116	0.6006
20	Img1	0.3472	0.3427	0.2971	0.4654	0.3163	0.1286
	Img2	0.3824	1.7523	0.3089	0.4261	0.5682	0.1432
	Img3	12.6460	1.9598	2.7243	3.0159	1.4341	2.7171
	Img4	0.6017	2.3836	0.4317	0.5692	0.6093	0.2761
	Img5	0.3827	0.5513	0.4618	0.8218	0.4369	0.5457
	Img6	1.0707	0.5798	2.9782	2.4591	0.7232	1.1108
	Img7	0.4296	0.4432	0.4131	0.6962	0.4200	0.3496
	Img8	0.4190	0.4399	0.4183	0.7330	0.4238	0.3882
	Img9	0.4187	0.4396	0.4160	0.5426	0.4194	0.2474
	Img10	0.4288	0.4502	0.4354	0.7329	0.4180	0.4498
	Img11	0.4232	0.4501	0.4221	0.6891	0.4420	0.4384
Mean		0.6599	0.6376	0.6081	0.8926	0.5726	0.6369

followed by FA (with 17 cases), SSO (with 16 cases), WOA (with 14 cases), VPL (with 12 cases), and SCA (with three cases).

The VPLWOA has obtained the high fitness values in most images in thresholds four, six, and 20 and performed equally with WOA and VPL in threshold two. In thresholds eight, 10, 16, and 18, VPLWOA performed nearly like WOA, VPL, SSO, and FA. The SSA is the worst

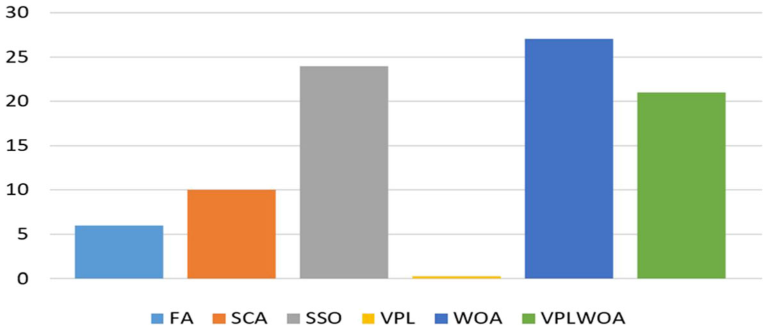

Fig. 9 CPU time ranking of all algorithms

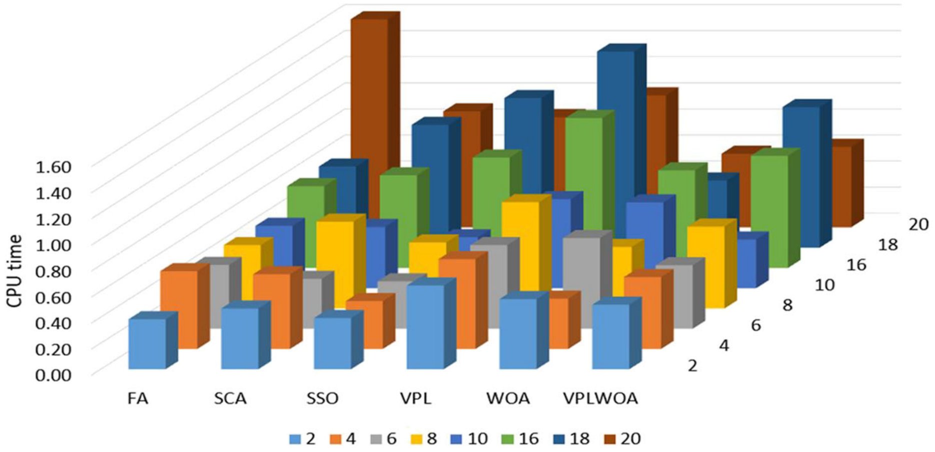

Fig. 10 Average CPU time for all algorithms at each threshold level

one among all the algorithms. Figure 8 shows the average of the fitness values for all algorithms at each threshold level.

Based on these results, VPLWOA outperformed the other algorithms with 30%, 26%, and 30% for PSNR, SSIM, and fitness value, respectively, thereby indicating that the VPL is improved using WOA as a local search.

For further analysis, the CPU time results for each algorithm are recorded in Table 4. From this table, the VPLWOA achieved the best results in 21 cases and is ranked third after both WOA (with 27 cases) and SSO (with 24 cases). The SCA obtained the fourth rank (with 10 cases) followed by the FA (with 6 cases), it was ranked fifth. Whereas, the VPL was considered as the slowest algorithm in the experiments. The VPLWOA showed good CPU time in a large threshold than the smallest one.

Moreover, the results can be summarized as in Fig. 9. This figure illustrates the CPU time ranking of the algorithms overall thresholds and images. Whereas Fig. 10 shows the average of CPU time for all algorithms at each threshold level.

4.4 Experimental series 2: medical images

In this experiment, the performance of the presented algorithm is assessed to determine the optimal threshold to segment a medical dataset. This dataset contains a set of lymphoblastic leukemia image database [27], which is classified into two groups (for more details, see [27]). The main task of this experiment is to segment the leukocytes (darker cells). However, this task is difficult because the blood cells do not have the same abnormalities that can influence the performance of the segmentation method. The VPLWOA is compared with the same algorithms used in previous experiments with the same parameter settings. Figure 11 shows the tested blood cell images with their histogram. These images have different characteristics.

The results of PSNR and SSIM measures of the VPLWOA method against the other methods are given in Table 5 and Figs. 12 and 13; whereas, Fig. 14 shows a sample of segmented Leukemia image and its histogram with corresponding thresholds at threshold level 8.

Concerning PSNR, the results illustrate that the VPLWOA has achieved the best results in 19 cases out of 48, followed by SSO with 14 cases; whereas, VPL and SCA

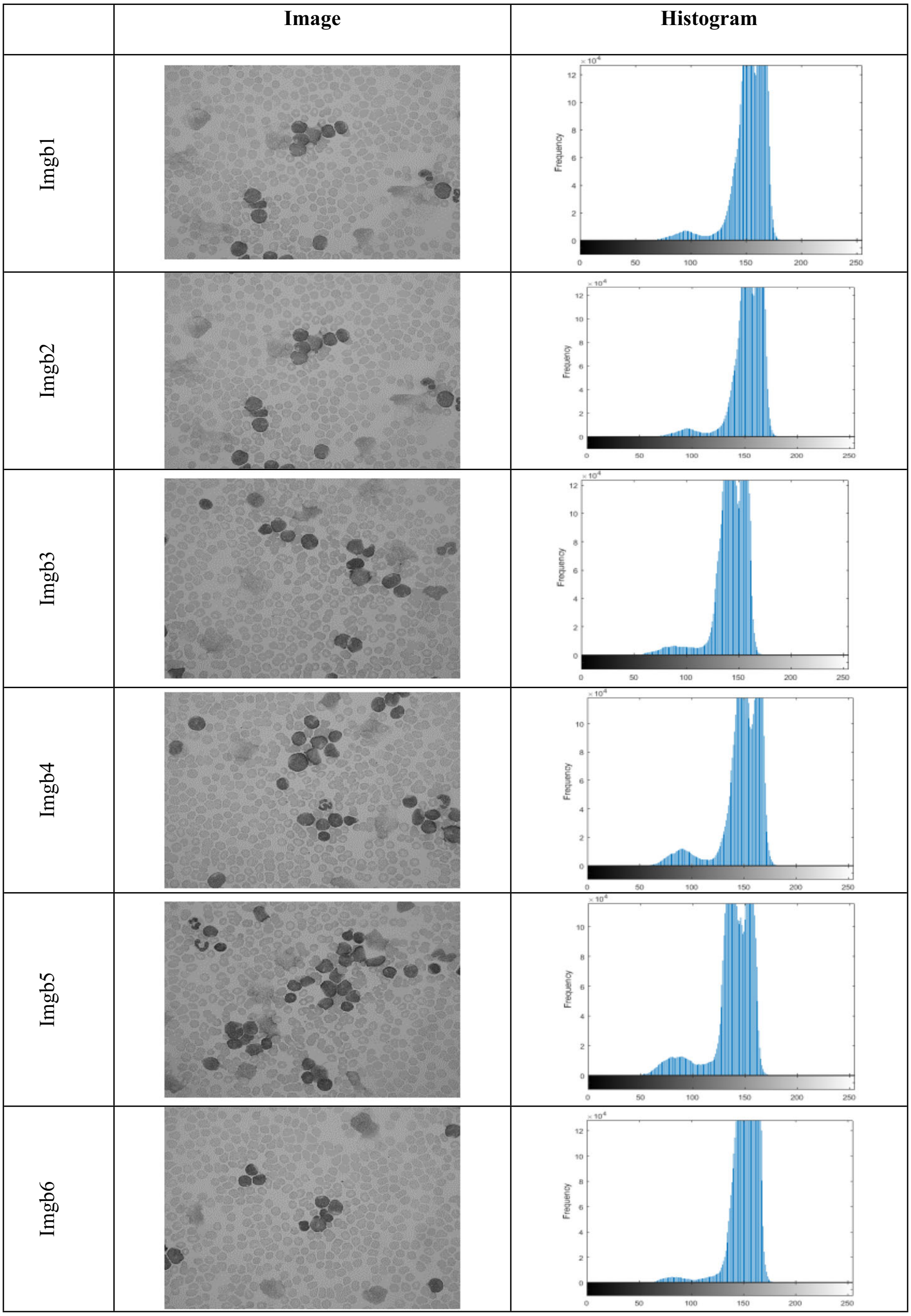

Fig. 11 Original and histogram of the blood cell images of leukemia image

obtained similar results (five cases for each one). The WOA came in the fifth rank with four cases, followed by FA with one case only. Moreover, the VPLWOA has the best PSNR values in threshold four and the highest threshold levels (i.e., eight, 10, 16, 18,

Table 5 Results of blood cell segmentation

	Threshold	FA	SCA	SSO	VPL	WOA	VPLWOA
PSNR	2	17.018	17.724	18.332	17.369	17.260	17.910
	4	19.567	19.913	19.813	20.220	19.093	20.492
	6	21.032	22.404	21.937	21.593	21.266	22.231
	8	21.828	21.563	23.976	21.878	23.738	24.384
	10	24.853	22.989	24.204	22.403	24.742	25.183
	16	23.764	24.578	26.263	23.356	25.584	26.406
	18	24.393	26.586	25.748	26.529	26.252	28.501
	20	25.439	28.892	27.065	26.098	27.757	31.292
	Mean	22.237	23.081	23.417	22.431	23.212	24.550
SSIM	2	0.744	0.775	0.760	0.760	0.740	0.769
	4	0.785	0.780	0.796	0.780	0.788	0.791
	6	0.800	0.805	0.801	0.804	0.792	0.802
	8	0.818	0.820	0.837	0.826	0.839	0.844
	10	0.846	0.824	0.832	0.815	0.799	0.855
	16	0.854	0.867	0.858	0.846	0.814	0.868
	18	0.868	0.844	0.848	0.855	0.845	0.887
	20	0.884	0.861	0.860	0.879	0.882	0.899
	Mean	0.8249	0.8220	0.8240	0.8206	0.8124	0.8394

and 20), while it came in the second rank in threshold levels two and six after SCA and SSO, respectively.

In terms of SSIM, the VPLWOA has obtained the best SSIM results in the highest threshold levels (i.e., eight, 10, 16, 18, and 20), while it came in the second rank in threshold levels two and six after SCA and four after SSO, as shown in Table 5.

Figure 12 illustrates the ranking of the algorithms overall thresholds and images for the PSNR and SSIM. As shown in this figure, the VPLWOA method is better than all other algorithms.

Besides, Fig. 13 depicts the average of PSNR and SSIM overall, the tested image at each threshold level. From this figure, it can be noticed the high ability of the proposed VLPWOA to find the optimal threshold value that improves the quality of the segmented image, and this reflected from the PSNR and SSIM values.

Based on the previous discussion, the proposed VPLWOA image segmentation outperforms the other methods. However, this approach has some limitations; for example, the time complexity needs to be improved, which can be decreased by enhancing the other phases of the VPL.

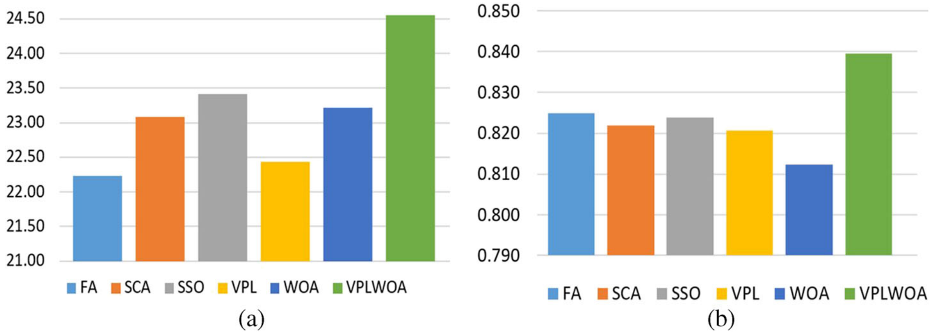

Fig. 12 Ranking of the (**a**) PSNR measure. (**b**) SSIM measure

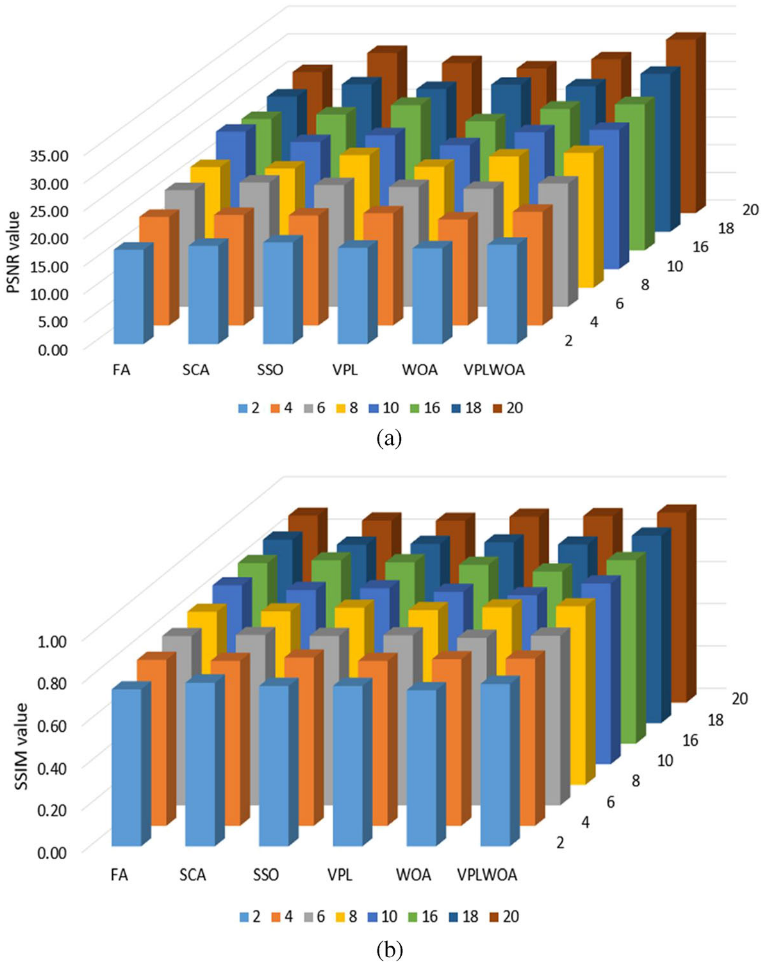

Fig. 13 Comparison between the VPLWOA and the other algorithms in terms of PSNR and SSIM in blood cell segmentation. **a** PSNR measure, **b** SSIM measure

In addition, the parameters of the VPL algorithm need a suitable value to be determined. More efficient methods, such grid search, can be used to solve this problem. In the future, we can evaluate the proposed method over different applications and fields such as image retrieval and feature selection; moreover, we can develop it to work with the salient object detection (SOD) methods. SOD works to save the most visually distinctive items in an image [15, 17, 52], which can effectively improve the segmentation results, especially with the blood cell image segmentation.

5 Conclusions

This study introduces an alternative multilevel image segmentation method. The proposed method is called VPLWOA, given that it uses the operators of WOA to

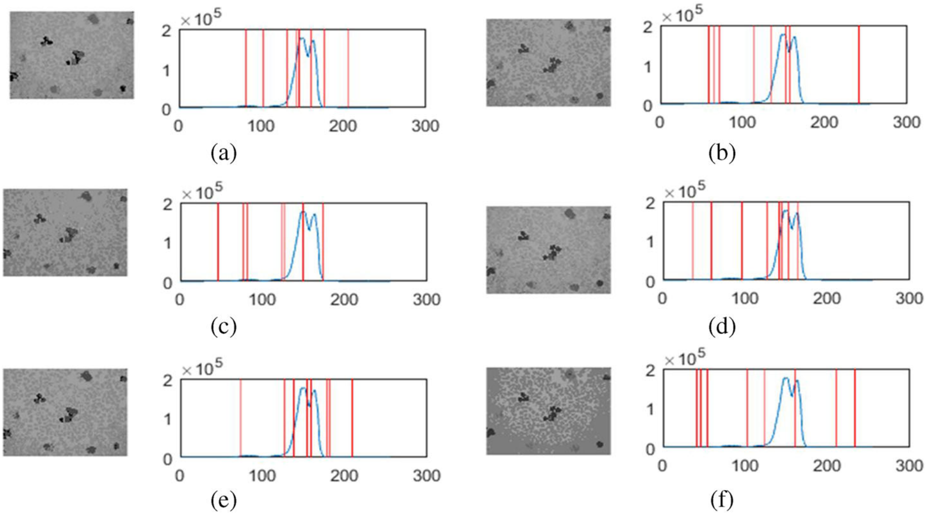

Fig. 14 Results of the histogram and corresponding thresholds over a segmented image at threshold eight. **a** FA, **b** SCA, **c** SSO, **d** VPL, **e** WOA, **f** VPLWOA

improve the learning phase of the traditional VPL algorithm. This phase has the main effect on the performance of the VPL. The proposed VPLWOA uses the histogram of the image as the input for maximizing the Otsu's function to find the best threshold to segment the given image. The performance of the proposed VPLWOA is verified through a set of experiments using two datasets, and the results are compared with SSO, SCA, FA, VPL, and WOA. The experimental results show that the proposed VPLWOA outperforms the other algorithms in terms of PSNR, SSIM, and fitness function.

According to the promising results, the proposed method can be used in many other applications and subjects in future, such as feature selection and improving the clustering and classification of galaxy images. Also, the method can be applied in cloud computing and big data optimization.

Acknowledgments This work is supported by the Hubei Provincinal Science and Technology Major Project of China under Grant No. 2020AEA011 and the Key Research & Developement Plan of Hubei Province of China under Grant No. 2020BAB100.

Compliance with ethical standards

Conflict of interest The authors declare that they have no conflict of interest.

Ethical approval This article does not contain any studies with human participants performed by any of the authors.

Informed consent Informed was obtained from all individual participants included in the study.

References

1. Ahmadi M, Kazemi K, Aarabi A et al (2019) Image segmentation using multilevel thresholding based on modified bird mating optimization. Multimed Tools Appl 78:23003–23027. https://doi.org/10.1007/s11042-019-7515-6
2. Akay B (2013) A study on particle swarm optimization and artificial bee colony algorithms for multilevel thresholding. Appl Soft Comput J 13:3066–3091. https://doi.org/10.1016/j.asoc.2012.03.072
3. Awada W, Khoshgoftaar TM, Dittman D, et al (2012) A review of the stability of feature selection techniques for bioinformatics data. Proc 2012 IEEE 13th Int Conf Inf Reuse Integr IRI 2012 356–363. https://doi.org/10.1109/IRI.2012.6303031
4. Baby Resma KP, Nair MS (2018) Multilevel thresholding for image segmentation using Krill Herd Optimization algorithm. J King Saud Univ - Comput Inf Sci. https://doi.org/10.1016/j.jksuci.2018.04.007
5. Bao X, Jia H, Lang C (2019) A novel hybrid Harris Hawks optimization for color image multilevel thresholding segmentation. IEEE Access 7:76529–76546. https://doi.org/10.1109/ACCESS.2019.2921545
6. Bhandari AK, Singh N, Shubham S (2019) An efficient optimal multilevel image thresholding with electromagnetism-like mechanism. Multimed Tools Appl 78:35733–35788. https://doi.org/10.1007/s11042-019-08195-8
7. Bohat VK, Arya KV (2019) A new heuristic for multilevel thresholding of images. Expert Syst Appl 117:176–203
8. Clerc M, Kennedy J (2002) The particle swarm — explosion , stability , and convergence in a multidimensional complex space. 6:58–73
9. El AMA, Ewees AA, Hassanien AE (2017) Whale optimization algorithm and moth-flame optimization for multilevel thresholding image segmentation. Expert Syst Appl 83:242–256. https://doi.org/10.1016/j.eswa.2017.04.023
10. El AMA, Ewees AA, Hassanien AE (2018) Multi-objective whale optimization algorithm for content-based image retrieval. Multimed Tools Appl 77:1–38. https://doi.org/10.1007/s11042-018-5840-9
11. Elaziz MA, Oliva D, Ewees AA, Xiong S (2019) Multi-level thresholding-based grey scale image segmentation using multi-objective multi-verse optimizer. Expert Syst Appl 125:112–129
12. Elaziz MA, Heidari AA, Fujita H, Moayedi H (2020) A competitive chain-based Harris Hawks Optimizer for global optimization and multi-level image thresholding problems. Appl Soft Comput:106347. https://doi.org/10.1016/j.asoc.2020.106347
13. Elaziz MA, Ewees AA, Yousri D et al (2020) An improved marine predators algorithm with fuzzy entropy for multi-level thresholding: real world example of COVID-19 CT image segmentation. IEEE Access 8:125306–125330. https://doi.org/10.1109/ACCESS.2020.3007928
14. Ewees AA, Abd Elaziz M, Al-Qaness MAA et al (2020) Improved artificial bee colony using sine-cosine algorithm for multi-level thresholding image segmentation. IEEE Access 8:26304–26315
15. Fan D-P, Cheng M-M, Liu J-J, et al (2018) Salient objects in clutter: Bringing salient object detection to the foreground. In: Proceedings of the European conference on computer vision (ECCV). pp 186–202
16. Farshi TR (2018) A multilevel image thresholding using the animal migration optimization algorithm. Iran J Comput Sci:1–14
17. Fu K, Zhao Q, IY-H G, Yang J (2019) Deepside: A general deep framework for salient object detection. Neurocomputing 356:69–82
18. Gao H, Fu Z, Pun CM, et al (2017) A multi-level thresholding image segmentation based on an improved artificial bee colony algorithm. Comput Electr Eng 0:1–8. https://doi.org/10.1016/j.compeleceng.2017.12.037
19. Gupta S, Deep K (2019) Improved sine cosine algorithm with crossover scheme for global optimization. Knowledge-Based Syst 165:374–406. https://doi.org/10.1016/j.knosys.2018.12.008
20. He L, Huang S (2017) Modified firefly algorithm based multilevel thresholding for color image segmentation. Neurocomputing 240:152–174. https://doi.org/10.1016/j.neucom.2017.02.040
21. Horng MH, Liou RJ (2011) Multilevel minimum cross entropy threshold selection based on the firefly algorithm. Expert Syst Appl 38:14805–14811. https://doi.org/10.1016/j.eswa.2011.05.069
22. Hussein WA, Sahran S, Sheikh Abdullah SNH (2013) A new initialization algorithm for bees algorithm. Commun Comput Inf Sci 378 CCIS:39–52. https://doi.org/10.1007/978-3-642-40567-9_4
23. Jia H, Peng X, Song W et al (2019) Multiverse optimization algorithm based on Lévy flight improvement for multithreshold color image segmentation. IEEE Access 7:32805–32844. https://doi.org/10.1109/ACCESS.2019.2903345
24. Kapur JN, Sahoo PK, Wong AK (1985) A new method for gray-level picture thresholding using the entropy of the histogram. Comput vision, Graph image Process 29:273–285
25. Khairuzzaman AKM, Chaudhury S (2017) Multilevel thresholding using grey wolf optimizer for image segmentation. Expert Syst Appl 86:64–76. https://doi.org/10.1016/j.eswa.2017.04.029

26. Kumar A, Konwer A, Kumar A et al (2019) Script identification in natural scene image and video frames using an attention based Convolutional-LSTM network. Pattern Recognit 85:172–184. https://doi.org/10.1016/j.patcog.2018.07.034
27. Labati RD, Piuri V, Scotti F (2011) All-Idb: the acute lymphoblastic leukemia image database For image processing Ruggero Donida Labati IEEE Member, Vincenzo Piuri IEEE Fellow, Fabio Scotti IEEE Member Universit ` a degli Studi di Milano, Department of Information Technologies,. IEEE Int Conf Image Process 2045–2048
28. Liang J, Wang L (2018) A fast SAR image segmentation method based on improved chicken swarm optimization algorithm
29. Ma L, Liu X, Gao Y et al (2017) A new method of content based medical image retrieval and its applications to CT imaging sign retrieval. J Biomed Inform 66:148–158. https://doi.org/10.1016/j.jbi.2017.01.002
30. Mirjalili S, Lewis A (2016) The whale optimization algorithm. Adv Eng Softw 95:51–67. https://doi.org/10.1016/j.advengsoft.2016.01.008
31. Mittal H, Saraswat M (2018) An optimum multi-level image thresholding segmentation using non-local means 2D histogram and exponential Kbest gravitational search algorithm. Eng Appl Artif Intell 71:226–235. https://doi.org/10.1016/j.engappai.2018.03.001
32. Moghdani R, Salimifard K (2018) Volleyball premier league algorithm. Appl Soft Comput J 64:161–185. https://doi.org/10.1016/j.asoc.2017.11.043
33. Naji Alwerfali HS, A. A. Al-qaness, Abd Elaziz M, et al (2020) Multi-level image thresholding based on modified spherical search optimizer and fuzzy entropy. Entropy 22:328. https://doi.org/10.3390/e22030328
34. Oliva D, Cuevas E, Pajares G et al (2014) A Multilevel thresholding algorithm using electromagnetism optimization. Neurocomputing 139:357–381. https://doi.org/10.1016/j.neucom.2014.02.020
35. Oliva D, Hinojosa S, Elaziz MA, Ortega-Sánchez N (2018) Context based image segmentation using antlion optimization and sine cosine algorithm. Multimed Tools Appl:1–37. https://doi.org/10.1007/s11042-018-5815-x
36. Otsu N (1979) A threshold selection method from gray-level histograms. IEEE Trans Syst Man Cybern 9:62–66. https://doi.org/10.1109/TSMC.1979.4310076
37. Ouadfel S, Taleb-Ahmed A (2016) Social spiders optimization and flower pollination algorithm for multilevel image thresholding: A performance study. Expert Syst Appl 55:566–584. https://doi.org/10.1016/j.eswa.2016.02.024
38. Park S, Hong K (2018) Video semantic object segmentation by self-adaptation of DCNN. Pattern Recognit Lett 112:249–255. https://doi.org/10.1016/j.patrec.2018.07.032
39. Reynolds AM, Smith AD, Reynolds DR et al (2007) Honeybees perform optimal scale-free searching flights when attempting to locate a food source. J Exp Biol 210:3763–3770. https://doi.org/10.1242/jeb.009563
40. Rodríguez-Esparza E, Zanella-Calzada LA, Oliva D et al (2020) An efficient Harris hawks-inspired image segmentation method. Expert Syst Appl 155:113428. https://doi.org/10.1016/j.eswa.2020.113428
41. Sarkar S, Das S, Chaudhuri SS (2015) A multilevel color image thresholding scheme based on minimum cross entropy and differential evolution. Pattern Recognit Lett 54:27–35. https://doi.org/10.1016/j.patrec.2014.11.009
42. Sharawi M, Zawbaa HM, Emary E et al (2017) Feature selection approach based on whale optimization algorithm. Ninth Int Conf Adv Comput Intell 2017:163–168. https://doi.org/10.1109/ICACI.2017.7974502
43. Sun G, Zhang A, Yao Y, Wang Z (2016) A novel hybrid algorithm of gravitational search algorithm with genetic algorithm for multi-level thresholding. Appl Soft Comput J 46:703–730. https://doi.org/10.1016/j.asoc.2016.01.054
44. Tan Z, Zhang D (2020) A fuzzy adaptive gravitational search algorithm for two-dimensional multilevel thresholding image segmentation. J Ambient Intell Humaniz Comput. https://doi.org/10.1007/s12652-020-01777-7
45. Tang K, Yuan X, Sun T et al (2011) An improved scheme for minimum cross entropy threshold selection based on genetic algorithm. Knowledge-Based Syst 24:1131–1138. https://doi.org/10.1016/j.knosys.2011.02.013
46. Touma HJ (2016) Study of the economic dispatch problem on IEEE 30-bus system using whale optimization algorithm. Int J Eng Technol Sci 5:11–18. https://doi.org/10.15282/ijets.5.2016.1.2.1041
47. Wang Y, Meng Q, Qi Q et al (2018) Region merging considering within- and between-segment heterogeneity: An improved hybrid remote-sensing image segmentation method. Remote Sens 10:1–26. https://doi.org/10.3390/rs10050781
48. Wunnava A, Naik MK, Panda R et al (2020) A novel interdependence based multilevel thresholding technique using adaptive equilibrium optimizer. Eng Appl Artif Intell 94:103836. https://doi.org/10.1016/j.engappai.2020.103836

49. Xing Z, Jia H (2020) An improved thermal exchange optimization based GLCM for multi-level image segmentation. Multimed Tools Appl 79:12007–12040. https://doi.org/10.1007/s11042-019-08566-1
50. Xing Z, Jia H (2020) Modified thermal exchange optimization based multilevel thresholding for color image segmentation. Multimed Tools Appl 79:1137–1168. https://doi.org/10.1007/s11042-019-08229-1
51. Xiong W, Xu J, Xiong Z et al (2018) Optik degraded historical document image binarization using local features and support vector machine (SVM). Opt - Int J Light Electron Opt 164:218–223. https://doi.org/10.1016/j.ijleo.2018.02.072
52. Zhao J-X, Liu J-J, Fan D-P et al (2019) EGNet: Edge guidance network for salient object detection. Proceedings of the IEEE International Conference on Computer Vision, In, pp 8779–8788

Publisher's note Springer Nature remains neutral with regard to jurisdictional claims in published maps and institutional affiliations.

Affiliations

Mohamed Abd Elaziz[1] • **Neggaz Nabil**[2] • **Reza Moghdani**[3] • **Ahmed A. Ewees**[4] • **Erik Cuevas**[5] • **Songfeng Lu**[6]

Neggaz Nabil
nabil.neggaz@univ-usto.dz

Reza Moghdani
reza.moghdani@gmail.com

Ahmed A. Ewees
ewees@du.edu.eg

[1] Department of Mathematics, Faculty of Science, Zagazig University, Zagazig, Egypt

[2] Faculté des mathématiques et informatique - Département d'Informatique- Laboratoire SIMPA, Université des Sciences et de la Technologie d'Oran Mohammed Boudiaf, USTO-MB, BP 1505, El M'naouer, 31000 Oran, Algeria

[3] Industrial Management Department, Persian Gulf University, Boushehr, Iran

[4] Department of Computer, Damietta University, Damietta, Egypt

[5] Departamento de Electrónica, Universidad de Guadalajara, CUCEI Av. Revolución 1500, 44430 Guadalajara, Mexico

[6] School of Cyber Science and Engineering, Huazhong University of Science and Technology, Wuhan 430074, China